



Instituto de Física Teórica  
Universidade Estadual Paulista

---

---

Tese de Doutorado

IFT-T.008/14

**Dynamical gluon masses in perturbative calculations at loop level:  
Towards an effective loop expansion for Quantum Chromodynamics**

Fátima Araujo Machado

Orientador

*Adriano A. Natale*

Novembro de 2014

## Agradecimentos

A meus pais, irmão e irmã, pelo apoio e amor incondicionais e essenciais. Espero conseguir sempre expressar o quão preciosos e queridos vocês são. À minha mãe, pela abertura e disposição em conhecer minha vida e quem sou, e participar disso com amor e carinho sem medida.

A todos os Araújo e Machados, prima(o)s, tia(o)s e avó(ô)s (mesmo os que nada ou pouco conheci em presença, mas que deixaram sinais de personalidade e criação na família). Aos Machados, pelo amor e carinho sempre presentes mesmo nas, e na superação das maiores tensões carregadas pelas gerações. Aos Araújo, pela referência do quão valiosa é a simplicidade, e de amor, doçura e generosidade infinitos.

A todos os amigos e conhecidos que de uma forma ou outra, mesmo que indiretamente ou por ocasiões corriqueiras, me mostraram formas de ser e ver que contribuíram para que eu tenha me tornado o que hoje sou – e que portanto continuam contribuindo. Em especial Camila, Thales, Amanda, Luciana, Henrique, Carlos D’Alkaine, Thiago gaúcho, Eduardo, Lara, Carol, Ricardo, Leo BR, Julia, dentre tantos outros.

Também àqueles que fizeram parte da minha vida e com quem pude contar. Mesmo tendo caminhos ou valores nos distanciados, meu carinho permanece.

A todas as contribuições e referências na minha construção pessoal, em particular Rádio UFSCar, CineUFSCar, Six Feet Under, B. Summers, Arcade Fire, Fiona Apple, Amanda Palmer, D. Bowie, L. Sakamoto, Mães de Maio, MTST, Marcelo Freixo, dentre muitos outros.

Aos companheiros de IFT Thales e Renann, pelas conversas e ajudas sempre disponíveis, e por terem tornado os dias mais agradáveis nesses anos de IFT. Aos físicos cariocas Mauricio, Reinaldo, Daniel, Daniela e Kroff, por tornarem os eventos mais produtivos e agradáveis.

Ao Henrique, por ter aberto e compartilhado suas vivências e um pouco do seu mundo em Lisboa, e por ser também uma referência de força e sensibilidade.

Ao “irmãozinho” Thales, por todas as ajudas incondicionais, pelas conversas das mais variadas e sempre boas. Por se dispor a ouvir de tudo e dar risada da vida. Pela companhia e por tanto acrescentar, desde almoços, lanches e glossário próprio a compreensão, paciência e à forma Thales de ser.

À Angela, pela Camila e por me receber sempre de braços abertos.

À Camila, pelo amor e parceria todos esses anos, e estar ao meu lado sempre. Por entender quando meu trabalho não deixou muito espaço para ser gente o tanto quanto poderia. Por compartilhar dos valores mais importantes, e ser uma pessoa aberta e incrível de se viver e crescer junto. Por sofrer ao lado e rir e sorrir junto. Por sempre me lembrar de dar maior importância ao que realmente importa, e ser uma referência de sensibilidade e de coragem pra se bancar quem se é.

Ao Banksy e ao Rolezinho, por adoçarem nossas vidas e entenderem (às vezes) quando a mãe não dá atenção ao trabalhar no ganha-ração-e-Pipicat.

Aos envolvidos no Congressinho 2012, em especial o Thales, os professores do IFT Vicente e Juan, e todos professores que participaram e fizeram da organização do evento uma atividade extremamente gratificante.

Aos professores que de uma ou outra forma foram influentes ou inspiradores na minha formação profissional. Gratidão eterna ao Zee pelo seu livro de QFT. À banca, pela participação e pela paciência e compreensão na finalização desta tese. A Rosane e Luzinete, sempre agradáveis e solícitas em tudo que precisei na secretaria do IFT.

E ao Adriano, pela orientação, discussões e paciência ao longo desses anos de mestrado e doutorado.

Finalmente a CAPES, CNPq e FAPESP pelo essencial apoio financeiro.

## Abstract

This thesis is based on part of the work done during the Ph.D., and it concerns the two distinguished domains of Quantum Chromodynamics (QCD) at zero temperature: the low-energy, confined domain, and the high-energy, asymptotically free one. Aiming to bridge the gap between them, and inspired by suggested improvements of the QCD perturbative series, this work investigates a proposal for an improved perturbative expansion, as a method to be applicable to QCD phenomenology, as well as to nonperturbative studies.

The proposal consists in an effective-loop expansion – a hybrid between Schwinger-Dyson equations and usual loop expansions, making use of the latter’s framework, yet dressing certain quantities in order to account for their complete behavior inside loops. The thesis describes the main efforts on this matter, in its application to correlation functions – the gluon and ghost propagators, in particular, as a preliminary step preceding further applications.

After dealing with issues as transversality of the gluon self-energy and renormalizability within the method, the present form of the effective-loop expansion contains dynamically massive gluons and an effective running charge, besides the possible dressing of the three-gluon vertex. Within this formulation, reasonable qualitative results were obtained for achieving the complete, nonperturbative behavior of the ghost and gluon propagators, and comparison with lattice is analyzed. Readily achievable and longer term prospects are also discussed.

**Keywords:** Quantum Chromodynamics. Dynamical gluon mass. Schwinger-Dyson equations. Dynamical Perturbation Theory.

## Resumo

A presente tese é baseada em parte do trabalho realizado durante o Doutorado e diz respeito aos dois domínios da Cromodinâmica Quântica (QCD) a temperatura zero: o regime confinado, a baixas energias, e o assintoticamente livre, a altas energias. Com o objetivo de cumprir uma ponte entre estes domínios e inspirado em sugestões de aprimoramentos da série perturbativa, este trabalho investiga uma proposta para uma expansão perturbativa aprimorada, a ser um método aplicável tanto à fenomenologia da QCD quanto a estudos de seu regime não-perturbativo.

A proposta consiste numa expansão em loops efetivos – um híbrido entre equações de Schwinger-Dyson e expansão em loops usual, fazendo uso de ferramentas desta porém vestindo certas quantidades como forma de considerar seu comportamento completo dentro de loops. A tese descreve os principais avanços nesse sentido, na aplicação a funções de correlação – em particular os propagadores do gluon e do ghost, como um passo preliminar a futuras aplicações.

Após lidar com questões de transversalidade do propagador do gluon e renormalizabilidade no método, a expansão em loops efetivos na sua presente forma contém gluons (dinamicamente) massivos e uma carga efetiva, além da possibilidade de uma vestimenta para o vértice de três gluons. Nesta formulação, foram obtidos resultados qualitativos razoáveis para o comportamento não-perturbativo completo dos propagadores do ghost e do gluon, e comparação com a rede é analisada. Perspectivas de curto e de mais longo prazo são discutidas.

**Palavras-chave:** Cromodinâmica Quântica. Massa dinâmica de gluons. Equações de Schwinger-Dyson. Teoria Dinâmica de Perturbação.

*Como é por dentro outra pessoa  
Quem é que o saberá sonhar?  
A alma de outrem é outro universo  
Com que não há comunicação possível,  
Com que não há verdadeiro entendimento.*

*Nada sabemos da alma  
Senão da nossa;  
As dos outros são olhares,  
São gestos, são palavras,  
Com a suposição de qualquer semelhança  
No fundo.*

Fernando Pessoa

*Soy lo que dejaron  
Soy toda la sobra de lo que se robaron  
Un pueblo escondido en la cima  
Mi piel es de cuero, por eso aguanta cualquier clima  
Soy una fábrica de humo  
Mano de obra campesina para tu consumo  
Frente de frío en el medio del verano  
El amor en los tiempos del cólera, mi hermano!  
  
Soy el desarrollo en carne viva  
Un discurso político sin saliva  
Las caras más bonitas que he conocido  
Soy la fotografía de un desaparecido  
La sangre dentro de tus venas  
Soy lo que me enseñó mi padre  
El que no quiere a su patria, no quiere a su madre  
Soy América Latina, un pueblo sin piernas, pero que camina*

Calle 13 (Latinoamerica)

*O rio que fazia uma volta atrás de nossa casa  
era a imagem de um vidro mole que fazia uma  
volta atrás de casa.*

*Passou um homem depois e disse: Essa volta  
que o rio faz por trás de sua casa se chama  
enseada.*

*Não era mais a imagem de uma cobra de vidro  
que fazia uma volta atrás de casa.*

*Era uma enseada.*

*Acho que o nome empobreceu a imagem.*

Manoel de Barros (O livro das Ignoranças)

# Contents

<b>1</b>	<b>Introduction</b>	<b>1</b>
1.1	The object of research . . . . .	1
1.2	Development of the theory . . . . .	2
1.2.1	The Quantum . . . . .	3
1.2.2	The Chromo . . . . .	4
1.2.3	And the dynamics . . . . .	5
1.3	The present work . . . . .	6
<b>2</b>	<b>Quantum Field Theory</b>	<b>8</b>
2.1	Basics . . . . .	8
2.1.1	Correlation functions . . . . .	9
2.1.2	Perturbative expansion . . . . .	11
2.1.3	The Schwinger-Dyson equations . . . . .	13
2.2	Renormalization . . . . .	16
2.2.1	Renormalized Lagrangians . . . . .	17
2.2.2	Renormalization Group . . . . .	18
<b>3</b>	<b>Quantum Chromodynamics</b>	<b>20</b>
3.1	Perturbative QCD . . . . .	20
3.1.1	From valence quarks to distribution functions . . . . .	20
3.1.2	Limitations of perturbative QCD . . . . .	22
3.2	Nonperturbative QCD . . . . .	23
3.2.1	Lattice and Schwinger-Dyson agreements . . . . .	24
3.2.2	Gluon mass and the strong coupling . . . . .	25
3.2.3	Pinch Technique . . . . .	26
3.3	Improvements of the perturbative series . . . . .	29
<b>4</b>	<b>Effective loop expansion</b>	<b>31</b>
4.1	The proposal . . . . .	31
4.1.1	First attempts and issues found . . . . .	31

4.1.2	Methodology . . . . .	32
4.2	Gluon and ghost propagators to 1 effective-loop . . . . .	33
4.3	Transversality of the gluon propagator . . . . .	35
4.4	Renormalization . . . . .	36
4.4.1	Nonperturbative renormalization . . . . .	38
4.4.2	Hybrid approach . . . . .	39
4.4.3	Renormalized Perturbation . . . . .	40
4.5	Further dressings: effective charge and running mass . . . . .	41
<b>5</b>	<b>Results</b>	<b>44</b>
5.1	Analytical expressions . . . . .	44
5.1.1	Gluon propagator . . . . .	44
5.1.2	Ghost propagator . . . . .	47
5.2	Successful renormalization schemes . . . . .	48
5.3	Comparison to lattice results . . . . .	51
5.3.1	Gluon propagator . . . . .	52
5.3.2	Ghost dressing . . . . .	55
5.4	Conclusions and prospects . . . . .	58
<b>A</b>	<b>Summary of the calculation procedure</b>	<b>59</b>
	<b>Bibliography</b>	<b>61</b>



# Chapter 1

## Introduction

### 1.1 The object of research

Physics aims, basically, to describe the domain of natural phenomena: how the things we see behave the way they do.

Along the centuries Physics managed to extend its meaning of “seeing”: with the accumulated knowledge, we can infer that a certain process must have happened, or that some system must have certain characteristics – even if we do not access them directly by any measurement means. That is, when there are only indirect evidences for them.

According with the current understanding of Cosmology, for instance, 24% of the Universe must be composed by what is called dark matter, and about 71% by dark energy, and one of their main properties is: we cannot observe them directly at all. Why then is it believed that they are there? Because, as far as the currently well-established knowledge goes, it all points to this conclusion, from observations that cannot be, or at least were not, explained otherwise. Given that, physicists then attempt to model such types of system to infer further effects that could be observed, thus indirectly corroborating their stand.

In fact, there is something similar with the other  $\sim 5\%$  of the Universe, which is the ordinary matter – the one we know to be made of atoms. Actually, of more fundamental particles: as molecules are made of atoms, these are an electrons-nucleus system, and nuclei are made of protons and neutrons, it does not stop here. Protons and neutrons are made of even more elementary parts. And it seems to stop there.

These parts are believed to be certain fundamental (i.e. indivisible and substructureless) particles: the quarks and the gluons. They are, as far as we currently know from experiments, the basic building blocks of our ordinary matter.

What happens is that no one has ever observed them, neither quarks nor gluons. Nevertheless, the accumulated knowledge on this type of system, from the well-established Quantum Theory, led to the conclusion that these particles should indeed be.

There being enough evidence, the physicists' work is then to formulate a precise theory of these quarks and gluons that will be able to predict the whole behavior observed in experiments with protons, neutrons and particles alike (v. Sect.1.2).

Moreover, one could think that this lack of direct observation is an empirical limitation, like, for example, how it was thought that no experiment could isolate and manipulate individual atoms, until technology did allow it.

However, the fact that we can access quarks and gluons only indirectly is unanimously [1] understood not to be a technical or experimental restriction, but being an intrinsic quality: It is not just that we cannot observe isolated quarks or gluons, but that they are never isolated: they do exist individually, but only bound to be together in some specific manners. This phenomenon is called *confinement*, and it must somehow be described by any theory that concerns quarks and gluons.

Yet more interesting, there is one correction to that: they are never isolated in the usual state of matter, i.e. in the subatomic particles we know of. For very high densities and temperatures, the quarks and gluons *deconfine* into another state of matter – which is the quark-gluon plasma (QGP). It is believed that the Universe, at some point near the Big Bang, was in a QGP, and this state has been produced in heavy ion accelerators, providing experimental access to this deconfinement transition, which is also an open problem in Physics, as well as the (zero-temperature) confinement one. The present work will concern only the latter, the zero-temperature confinement presented by the usual state of ordinary matter.

## 1.2 Development of the theory

First of all, some terminology: as processes were studied, Physics established a classification of the fundamental interactions in nature. Besides gravitational force, there are the electromagnetic and the weak – later unified into the electroweak force, and, finally, the strong one. The electroweak and the strong forces are the ones involved\* in the physics of elementary particles, and we should note that the distinction between them came along with the history of experiments.

So the first terminology is the following: the particles that participate in the strong interactions are called *hadrons*, while the ones that do not so are called *lep-*

---

\*Up to the present, gravitation at small (quantum) scales is an open problem.

*tons*. For example, electrons, muons, neutrinos are leptons, while protons, neutrons, pions are hadrons [1].

The ruling theory for quarks and gluons is Quantum Chromodynamics (QCD), and its purpose is to describe the very being of hadrons, and also their properties and behavior.

Basically, we will spend this Section explaining what the name Quantum Chromodynamics means.

### 1.2.1 The Quantum

Although there is a **lot** about it, one can say that Quantum Mechanics (QM) is nothing but the physics of small scales – from the order of atomic sizes and below. That is, the dynamics of systems with the size of atoms or smaller are governed by QM, just like the dynamics of greater systems (like the ones we daily see and touch) are governed by Classical Mechanics, with Newton’s laws and so on.

So, describing the physics of microscopic scales and accounting for the atomic spectrum, and interactions between electrons and nuclei, QM consists in the theoretical framework for the understanding of (ordinary) matter [2]. Furthermore, it was seen that the QM rules should also apply to radiation [3], approximating the concepts of matter and radiation.

This development was later accompanied by the Dirac’s work on making QM compatible with Special Relativity [4], which led to a great advance: it predicted the existence of particles and antiparticles. At the time it was seemingly strange, but it was soon confirmed by experiment [5] and became a well-established and fundamental property of matter.

In fact, the smaller the scales physicists achieved to access, the more they observed processes characterized by transformation of some particles into others, as those involved in nuclei decays, for instance. Therefore, a theoretical framework that accounts for the appearance and disappearance of particles is able to describe such processes.

In the next chapter, we will describe this theoretical framework in its evolved form, that is Quantum Field Theory (QFT). For now, we proceed speaking of particles.

### 1.2.2 The Chromo

Sticking with the hadrons, experiments observed increasing types of them, building up the hadronic spectrum<sup>†</sup> – which is just like the atomic periodic table, but for more fundamental particles, deeper into the matter we know. Indeed, the hadron spectrum is a set of particles supposed to share the same kind of substructure, and substructure generally implies more fundamental degrees of freedom, i.e. implies even more fundamental particles.

It was in 1964 that Gell-Mann and (independently) Zweig proposed the quarks as constituents of this substructure. The original quark model contained three kinds of quarks, then called flavors: *up* ( $u$ ), *down* ( $d$ ), and *strange* ( $s$ ). Then, the hadrons were classified as mesons, made of a quark and an antiquark (a  $q\bar{q}$  system), or baryons, made of three quarks ( $qqq$ ), and the quark model accounted well for hadronic spectrum, that followed the patterns shown in Figures 1.1 and 1.2.

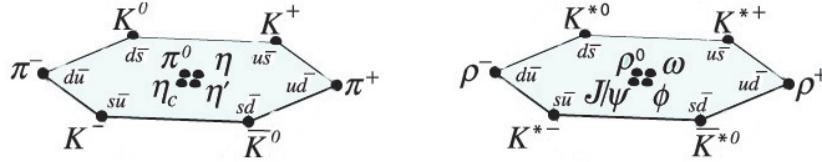


Figure 1.1: Meson spectrum for  $u$ ,  $d$ , and  $s$  quarks. The Figure, taken from [1], shows the mesons' quark composition and given names.

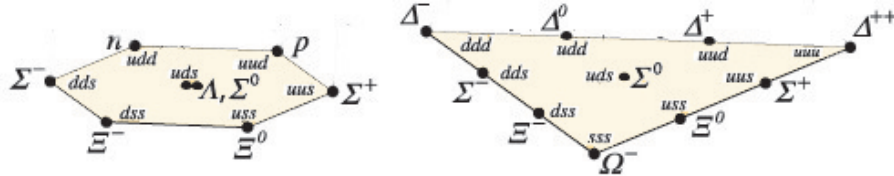


Figure 1.2: Baryon spectrum for  $u$ ,  $d$ , and  $s$  quarks. The Figure, taken from [1], shows the baryons' names and quark composition.

In a short time the three-flavor quark model was extended to contain a fourth flavor, the *charm* ( $c$ ), which was empirically evidenced in 1974. Later, two more quarks were proposed in the model, the *bottom* ( $b$ ) and the *top* ( $t$ ). The former was evidenced in 1977, and the top only in 1995, due to its large mass.

Now, consider a baryon with three identical quarks, like  $\Delta^{++}$  or  $\Delta^-$ . Since it is a fermion, its wave function should be anti-symmetric, but all of its observed

<sup>†</sup>For this history and further details we refer to [5, 6].

properties yielded a symmetric one. This led to the hypothesis that there would be an additional degree of freedom, even if unobserved, so that the particle's wave function could be:  $|qqq\rangle_A = |\text{space, spin, flavor}\rangle_S \times |\text{else}\rangle_A$ , with the subscript  $S(A)$  denoting (anti-)symmetric state.

This additional degree of freedom is precisely the color. Further evidence for it came, for example, with the ratio between cross-sections

$$R = \frac{\sigma(e^-e^+ \rightarrow \text{hadrons})}{\sigma(e^-e^+ \rightarrow \mu^-\mu^+)},$$

evaluated to be  $R \propto \sum_f Q_f^2$ , where the sum is over the quark flavors, each with charge  $Q_f$ . It was found that good agreement with experimental data is obtained with a proportionality factor near 3<sup>‡</sup>.

Then, if this factor is due to an internal degree of freedom, the color, it seems to be equally common to all flavors, and the data indicates it to assume three possible configurations. This means that quarks present a color symmetry, and it is formalized by the group  $SU(3)$ <sup>§</sup>.

### 1.2.3 And the dynamics

Symmetry principles had become one of the greatest paradigms in modern Physics. The statement of Noether's First Theorem that continuous global symmetries lead to conservation laws [7] gave founded description of observables in a Field Theory.

Noether's Second Theorem [8] for local symmetries, on the other hand, provided physicists with the gauge principle: according to it, the promotion of a global symmetry to a local one dictates the system's dynamics, that is, the form of the interactions in it.

So, it is by implementing this gauge principle to the color symmetry that one obtains QCD. It describes the quarks' interactions as being mediated by other particles – the gluons (whose presence in hadrons were also indicated by experiments [9]). That is, quarks interact by exchanging gluons, just like two electrons, for example, interact by exchanging photons in (quantum) Electrodynamics.

---

<sup>‡</sup>Similar considerations for the pion decay into two photons, and for anomaly cancellation in the Standard Model, are also successful with a corresponding factor  $\sim 3$ .

<sup>§</sup>Hadrons consist in the singlet representations of this symmetry, which means that all hadrons are “white” states, so that color is not observable.

### 1.3 The present work

In the mainstream literature, the gluon is said to be a massless particle, since it is so to any finite order in perturbation. Currently, though, nonperturbative studies of the gluon propagator lead to the conclusion that it would display a massive character, through the phenomenon of dynamical mass generation.

This phenomenon is understood to occur for both quarks and gluons, so that their dynamical masses are resultant from their interactions: in fact, all indications point that, generally, the masses of hadrons (therefore most of the mass of ordinary matter) do come from these interactions, somehow as the binding energy among its constituents. However, whether a consistent description of this binding is realizable with relation to the dynamical quark and gluon masses is also an open question.

On the other hand, understanding of the transition from the asymptotically free (v. Sect.3.1), high-energy domain to the confined, low-energy one also still lacks, while much of the experimental access to the theory relies on perturbative QCD, which, although having some well-established ground, still requires a model-dependent machinery.

The aim of this research is to contribute to bridging this gap between perturbative and nonperturbative QCD by means of an improved perturbative expansion, inspired by the Dynamical Perturbation Theory proposed some years ago [10, 11].

We investigate the construction of effectively dressed loop expansions, with the perspective for the future formulation of a loopwise dressed expansion with improved convergence and wider domain of validity, linking QCD's two domains by accessing deeper into the infrared (IR) one.

It is, thus, rather a method than a model: we propose an effective loop expansion which employs certain dressed quantities, in this way implementing nonperturbative characteristics of the theory's correlation functions *inside the loops*, so as to *account for their particular all-range fluctuations*.

In addition, we want this effective expansion to be applicable to QCD phenomenology, and, as the conciliation of a formally based method with phenomenological applicability can be even further away from a few-years future, we have opted for simplicity – which is twofold: First, concerning the expansion itself, we have guided ourselves to employ the fewer IR characteristics, and in one simplest manner as possible, to compose the sought-after improved expansion at 1 loop level. The second simplification lies in the objects we apply this expansion to: Yang-Mills (YM) correlation functions. This thesis presents, in particular, the gluon and the

ghost<sup>¶</sup> propagators.

The first idea was for the expansion to contain just dressed, massive gluons in loops. However, as will be described along this thesis, the progress of the research led us to consider two further ingredients: one is a running, effective charge which was also proposed by Cornwall [11, 12] and had been successfully applied to phenomenological calculations [13], consistently with dynamically massive gluons. The other is a dressing for the three-gluon vertex, in order to guarantee the transversality of the gluon self-energy – at least for one specific case, namely the background gluon self-energy.

The earliest attempts in this work are presented in [14], and briefly described in Subsect.4.1.1. Further developments and applications to YM vertices are in progress [15] and will be submitted to publication in a near future.

During the Ph.D., a similar introduction of dressed propagators was applied to chiral symmetry breaking [16] and to technicolor [17], involving a distinct effective propagator for the gluon [18] which supposedly contains intrinsic nonperturbative features.

Nevertheless, the earlier attempts on this effective expansion for YM Green functions led us to persist on this effort, to which the whole subsequent time of the Ph.D. was dedicated, and whose main advances this thesis aims to present. In Chap.2 we introduce some basics of QFT, while in Chap.3 we present, besides some basics of QCD, results and approaches of relevance and influence for our proposal, which is described and analyzed in Chap.4. Finally, the results for the gluon and ghost propagators are presented and analyzed in Chap.5, where we also describe the future prospects for continuation of this research.

Finally, before we start, we should set the basic conventions  $c = \hbar = 1$ . That is, speeds are measured in units of the speed of light (in vacuum), and actions are measured in units of the Planck constant (over  $2\pi$ ), and quantities may be equivalently written in powers of units of mass, energy, momentum or length.

---

<sup>¶</sup>Introductory note: ghosts are parameterizations of extra, unphysical degrees of freedom that are present in the theory due to its gauge symmetry. The combination of ghost and gluons are to represent the actual gauge degrees of freedom.

## Chapter 2

# Quantum Field Theory

This chapter concerns some generalities on QFT, and sets some conventions that were used in the present work. For details and further topics, we refer to [19, 20, 21]. Also, Zee’s outstanding book [22] is highly recommended for absolutely any topic that it covers.

To start, we borrow its very first phrase: “QFT arose out of our need to describe the ephemeral nature of life.”

Indeed, QFT is an appropriate language to describe the dynamics of creation and annihilation of degrees of freedom, and therefore, from the discussion in Chap.1, is suitable for particle physics.

### 2.1 Basics

Basically speaking, field theory deals with dynamic variables distributed throughout some space. For this reason, and despite its emergence from the conciliation between QM and Special Relativity, QFT is employed in both condensed matter and particle physics, and treated in general as nonrelativistic, or relativistic, respectively. So, plainly stating, QM is just a QFT in a zero-dimensional space [22].

As in a quantum theory, the dynamics of a system is described by its **S**-matrix, which is determined by the Hamiltonian and gives the transition amplitudes

$$\langle \text{out} | \text{in} \rangle \equiv \langle \text{in} | \mathbf{S} | \text{in} \rangle .$$

So, since our work concerns correlation functions, we first sketch how they are related to these transition amplitudes, and therefore relatable to physical observables.

The first hypothesis is the asymptotic (adiabatic) condition: that the above states are generated, from an unique vacuum state  $|\Omega\rangle$ , by the Heisenberg field



$\varphi(x)$  which satisfies

$$\lim_{x_0 \rightarrow \mp\infty} \langle \alpha | \varphi(x) | \beta \rangle = Z^{1/2} \langle \alpha | \varphi_{\text{out}}^{\text{in}}(x) | \beta \rangle \quad (2.1)$$

for all  $|\alpha\rangle, |\beta\rangle$  eigenstates of the free field  $\varphi_{\text{in}}(x) = \mathbf{S} \varphi_{\text{out}}(\mathbf{x}) \mathbf{S}^{-1}$ . The multiplicative factor  $\sqrt{Z}$  is just the component of  $\varphi(x) |\Omega\rangle$  along  $\varphi_{\text{in}}^{\text{out}}(x) |\Omega\rangle$ .

As a consequence, any transition amplitude between on-shell momentum eigenstates is related to the correlation functions of the field  $\varphi(x)$ ,

$$G^{(n)}(x_1, \dots, x_n) := \langle \Omega | T[\varphi(x_1) \cdots \varphi(x_n)] | \Omega \rangle, \quad (2.2)$$

where  $T$  is the time-ordering operator. This relation is the so-called reduction\* formula:

$$\begin{aligned} \langle p_1, \dots, p_n \text{ out} | q_1, \dots, q_l \text{ in} \rangle &= \left( \frac{i}{\sqrt{Z}} \right)^{n+l} \int \mathbf{d}^D x_1 \cdots \mathbf{d}^D y_n e^{i(\sum_{j=1}^n p_j \cdot y_j - \sum_{k=1}^l q_k \cdot x_k)} \times \\ &\quad \times (\square_{x_1} + m^2) \cdots (\square_{y_n} + m^2) G^{(n)}(y_1, \dots, y_n, x_1, \dots, x_l) \\ &\quad + \text{disconnected terms}, \end{aligned} \quad (2.3)$$

where  $m^2 = p_j^2 = q_k^2 \forall j, k$ , and the disconnected terms are those in which at least one particle in the process is not affected by it (i.e. with identical initial and final states).

By means of this relation, the computation of transition amplitudes amounts to determining correlation functions of the interacting theory, which we proceed to explore.

### 2.1.1 Correlation functions

In the path integral formalism of a  $D$ -dimensional QFT described by the Lagrangian  $\mathcal{L}[\varphi(x)]$  (its action denoted  $S[\varphi(x)]$ ), the vacuum expectation value (2.2) in the presence of a source  $J(x)$  is given by the functional integral over the dynamic variables

$$\begin{aligned} \mathcal{Z}[J] &\equiv \langle \Omega, \text{out} | \Omega, \text{in} \rangle_J \\ &= \int \mathcal{D}\varphi \exp i \left( S[\varphi(x)] + \int \mathbf{d}^D x J(x) \varphi(x) \right) \end{aligned} \quad (2.4a)$$

$$= \mathcal{Z}[0] \sum_{n=0}^{\infty} \frac{i^n}{n!} \int \mathbf{d}^D x_1 \cdots \mathbf{d}^D x_n J(x_1) \cdots J(x_n) G^{(n)}(x_1, \dots, x_n) \quad (2.4b)$$

$$\implies G^{(n)}(x_1, \dots, x_n) = \frac{1}{\mathcal{Z}[0]} \left. \frac{\delta^n \mathcal{Z}[J]}{i \delta J(x_1) \cdots i \delta J(x_n)} \right|_{J=0}, \quad (2.5)$$

---

\*or LSZ, for H. Lehmann, K. Symanzik, and W. Zimmermann [23].

whose Fourier transforms are the Green functions in momentum space:

$$(2\pi)^D \delta^D (p_1 + \dots + p_n) G^{(n)} (p_1, \dots, p_n) .$$

For Grassmann fields we define the even order Green functions as

$$G^{(2n)} (x_1, \dots, x_n, y_1, \dots, y_n) := \left( \frac{\delta}{i\delta\bar{\eta}(x_1)} \dots \frac{\delta}{i\delta\bar{\eta}(x_n)} \frac{i\delta}{\delta\eta(y_1)} \dots \frac{i\delta}{\delta\eta(y_n)} \mathcal{Z} [\eta, \bar{\eta}] \right) \Big|_{\eta, \bar{\eta}=0} . \quad (2.6)$$

Connected Green functions<sup>†</sup> are generated by the functional  $\mathcal{W} [J] := -i \log \mathcal{Z} [J]$ :

$$G_c^{(n)} (x_1, \dots, x_n) := \frac{\delta^n \mathcal{W} [J]}{\delta J (x_1) \dots \delta J (x_n)} \Big|_{J=0} , \quad (2.7)$$

whose Legendre transform is the effective action [21]

$$\Gamma [\phi] := \left[ \mathcal{W} [J] - \int d^D x J (x) \phi (x) \right] \Big|_{J(x)=J(x,\phi)} , \quad (2.8)$$

where

$$\phi (x, J) := \frac{\delta \mathcal{W} [J]}{\delta J (x)} = \frac{\langle \Omega | \varphi (x) | \Omega \rangle_J}{\langle \Omega | \Omega \rangle_J} , \quad (2.9)$$

is the vacuum expectation value (VEV) of  $\varphi(x)$  in the presence of the source  $J(x)$ .

Consequently

$$\frac{\delta \Gamma [\phi]}{\delta \phi (x)} = -J (x, \phi) , \quad (2.10)$$

which is the quantum version of the classical equation of motion,  $\delta S / \delta J = -J$  but in the quantum case  $\Gamma [\phi]$  contains all fluctuations that are embedded in the path integral:

$$\mathcal{Z} [J] = \int \mathcal{D}\varphi \exp i (S [\varphi] + J \cdot \varphi) = \exp i (\Gamma [\phi] + J \cdot \phi)$$

The effective action  $\Gamma [\phi]$  generates the proper vertices, also known as 1-particle irreducible (1PI) correlation functions. Going to momentum space:

$$\Gamma^{(n)} (p_1, \dots, p_n) := i^n \frac{\delta^n \Gamma [\phi]}{\delta \phi (p_1) \dots \delta \phi (p_n)} \Big|_{\phi=0} , \quad (2.11)$$

where the convention is that *all*  $p_i$  are *in-going* momenta in the Feynman diagram for the  $n$ -point proper vertex. We also follow the convention that *the given Feynman diagram corresponds to*  $i^{-n} \Gamma^{(n)}$  – that is, correspond to the functional derivatives, no  $i$  factors.

---

<sup>†</sup>They are related to processes in which no subsets of particles interact independently from each other, and are given by Feynman diagrams which are not separable in two or more disjoint ones.

Finally, from the very definition of the field  $\phi$ ,

$$\frac{\delta}{\delta\phi(y)} \frac{\delta\mathcal{W}[J]}{\delta J(x)} = \delta^D(x-y) ,$$

it follows the inverse relation between the 2-point proper vertex and the propagator:

$$-\Gamma^{(2)}(p, -p) = (iG_c^{(2)}(p, -p))^{-1} , \quad (2.12)$$

valid for commuting as well as for Grassmann fields.

Both Green functions above contain the quantum fluctuations of the theory, which is basically what we aim to study. So now we briefly describe how the perturbative expansion and the Schwinger-Dyson equations for such Green functions are constructed.

### 2.1.2 Perturbative expansion

When distinguishing in a Lagrangian the free and the interacting terms,  $\mathcal{L} = \mathcal{L}_0 + \mathcal{L}_i$  respectively, one can write:

$$\begin{aligned} \mathcal{Z}[J] &= \int \mathcal{D}\varphi \left( \exp i \int d^D x \mathcal{L}_i[\varphi] \right) \exp i \int d^D x \{ \mathcal{L}_0[\varphi] + J\varphi \} \\ &= \left( \exp i \int d^D x \mathcal{L}_i \left[ \frac{\delta}{i\delta J} \right] \right) \int \mathcal{D}\varphi \exp i \int d^D x \{ \mathcal{L}_0[\varphi] + J\varphi \} , \end{aligned} \quad (2.13)$$

where  $\mathcal{L}_0$  is related to a differential operator  $K$ , invertible by hypothesis, through (up to surface terms):

$$\int \mathcal{D}\varphi \exp i \int d^D x \{ \mathcal{L}_0 + J\varphi \} \propto \exp \frac{-i}{2} \int d^D x d^D y J(y) K^{-1}(y, x) J(x) .$$

Since  $\mathcal{Z}[J]$  is defined up to any multiplicative factor (see Eq.2.5), (2.13) becomes

$$\mathcal{Z}[J] = \exp \left( i \int d^D x \mathcal{L}_i \left[ \frac{\delta}{i\delta J} \right] \right) \exp \left( \frac{-i}{2} \int d^D x d^D y J(y) K^{-1}(y, x) J(x) \right) , \quad (2.14)$$

and then, by expanding the exponential series of  $\mathcal{L}_i[\delta/i\delta J]$ , one obtains, for any Green function, a perturbative expansion in the coupling constant(s) contained in  $\mathcal{L}_i$ .

The corresponding expansion for the effective action leads to a formal series in powers of the Planck constant  $\hbar$ , as well as a series in the coupling(s). Either way, one then obtains the usual perturbative, loop expansion of the quantum fluctuations of the field theory [19]<sup>‡</sup>.

---

<sup>‡</sup>Specifically, Sect.9-2-2.

For QCD, starting with the (unrenormalized) Lagrangian [24, 25]

$$\mathcal{L} = -\frac{1}{4}F^2 + \bar{\psi}^j (i \not{D} - m_j) \psi^j + (\partial^\mu \bar{c}^a) (D_\mu c^a) + \frac{1}{2\xi} (\partial_\mu A^{a\mu}) (\partial_\nu A^{a\nu}) , \quad (2.15)$$

$$\begin{aligned} &= -\frac{1}{4}(\partial_\mu A_\nu - \partial_\nu A_\mu) (\partial^\mu A^\nu - \partial^\nu A^\mu) + \frac{ig}{2} (\partial_\mu A_\nu - \partial_\nu A_\mu) [A^\mu, A^\nu] + \frac{g^2}{4} [A_\mu, A_\nu] [A^\mu, A^\nu] \\ &\quad + \bar{\psi}^j (i \not{D} - m_j) \psi^j + g\bar{\psi}^j \not{A}_\mu \psi^j + (\partial^\mu \bar{c}) (\partial_\mu c) - ig (\partial^\mu \bar{c}) [A_\mu, c] + \frac{1}{2\xi} (\partial \cdot A)^2 , \end{aligned} \quad (2.16)$$

the perturbative expansion of (2.14) yields loop expansions like the example below for the gluon propagator.

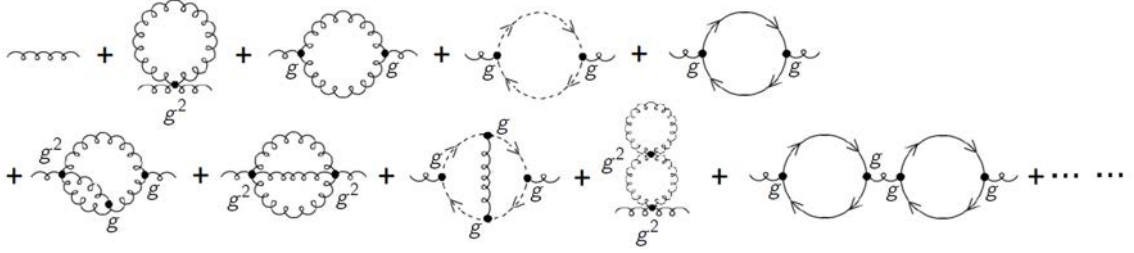


Figure 2.1: Perturbative expansion for the gluon propagator, up to two loops, showing the corresponding orders in  $g^0$  (tree-level),  $g^2$  and  $g^4$ .

Following given Feynman rules, one can generate the expansion for any Green function of the theory, to any finite order – i.e. up to any given number of loops.

These sums can be structured in terms of 1PI functions, as in the Figure below. All quantum fluctuations are contained in the full propagator,  $iG$ , represented by a blank circle, that is the sum of its tree-level part,  $iG^{(0)}$ , with the connected series of the 1PI corrections – called the self-energy,  $\Sigma$ , and represented by a shaded circle.

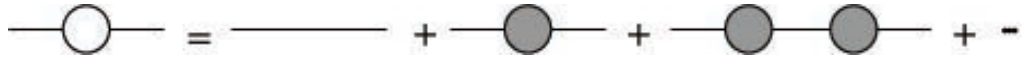


Figure 2.2: Dyson series for the gluon propagator: the full propagator as a connected series of the 1PI self-energy.

The self-energy is related to full the 2-point proper function,  $-\Gamma$ , by:

$$-\Gamma \equiv -\Gamma^{(0)} - \Gamma' \quad (2.17a)$$

$$= -\Gamma^{(0)} + \Sigma , \quad (2.17b)$$

where  $-\Gamma^{(0)}$  is its tree-level part, and  $-\Gamma'$  represents the corrections (the minus signs just follow the convention introduced in Subsect.2.1.1). Summing up the whole

Dyson series above amounts to the relation (2.12) between the propagator and the 2-point vertex:

$$-\Gamma = (iG)^{-1} \equiv (iG^{(0)})^{-1} + \Sigma \quad (2.18a)$$

$$= -\Gamma^{(0)} - \Gamma' , \quad (2.18b)$$

whose diagrammatic representation is given below in Figure 2.3. While connected functions are represented with blank circles, proper vertices are represented by black ones.

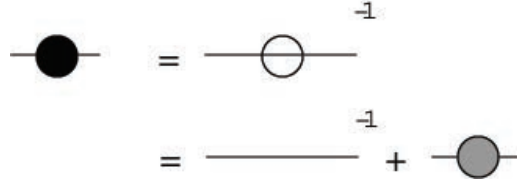


Figure 2.3: Diagrammatic representation of relation (2.17) between the full 2-point vertex and the full propagator, and their decomposition into tree-level and self-energy parts.

The self-energy can be treated, in principle, to any given order perturbatively, but it can also be given in terms of other full correlation functions of the theory. In the following subsection we explain what we mean by that.

### 2.1.3 The Schwinger-Dyson equations

Starting with the hypothesis that the identity

$$\int \mathcal{D}\varphi \frac{\delta}{\delta\varphi} \equiv 0 \quad (2.19)$$

holds in the theory under consideration,

$$\implies -i \int \mathcal{D}\varphi \frac{\delta}{\delta\varphi} \exp i \int \mathbf{d}^D x (\mathcal{L} + J\varphi) = \int \mathcal{D}\varphi \left[ \frac{\delta\mathcal{L}}{\delta\varphi}(\varphi) + J \right] \exp i \int \mathbf{d}^D x (\mathcal{L} + J\varphi) = 0 .$$

Considering  $\frac{\delta\mathcal{L}}{\delta\varphi}$  as a functional of the derivative  $\frac{\delta}{i\delta J(x)}$ :

$$\begin{aligned} \left[ \frac{\delta\mathcal{L}}{\delta\varphi} \left( \frac{\delta}{i\delta J(x)} \right) + J(x) \right] \mathcal{Z}[J] &= \int \mathcal{D}\varphi \left[ \frac{\delta\mathcal{L}}{\delta\varphi} \left( \frac{\delta}{i\delta J(x)} \right) + J(x) \right] \exp i \int \mathbf{d}^D x (\mathcal{L} + J\varphi) \\ &= \int \mathcal{D}\varphi \left[ \frac{\delta\mathcal{L}}{\delta\varphi}(\varphi) + J \right] \exp i \int \mathbf{d}^D x (\mathcal{L} + J\varphi) . \end{aligned}$$

$$\therefore \left[ \frac{\delta\mathcal{L}}{\delta\varphi} \left( \frac{\delta}{i\delta J(x)} \right) + J(x) \right] \mathcal{Z}[J] = 0 . \quad (2.20)$$

So, by applying further functional derivatives, as

$$\frac{\delta}{\delta J(y)} \left\{ \left[ \frac{\delta \mathcal{L}}{\delta \varphi} \left( \frac{\delta}{i\delta J(x)} \right) + J(x) \right] \mathcal{Z}[J] \right\} = 0, \quad (2.21)$$

one obtains integral equations coupling various (full) correlation functions of the theory. These are the Schwinger-Dyson equations (SDEs). We will explore their meaning now, and for that it suffices to exemplify diagrammatically some SDEs for QCD.

First, the SDE for the ghost propagator is given by:

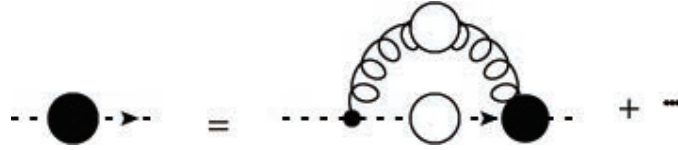


Figure 2.4: The SDE for the ghost propagator. Blank circles represent connected functions, and black ones, proper vertices.

So, the full (or dressed) ghost propagator is related to both the full gluon propagator and the full ghost-gluon vertex. For the gluon, the SDE corresponds to:

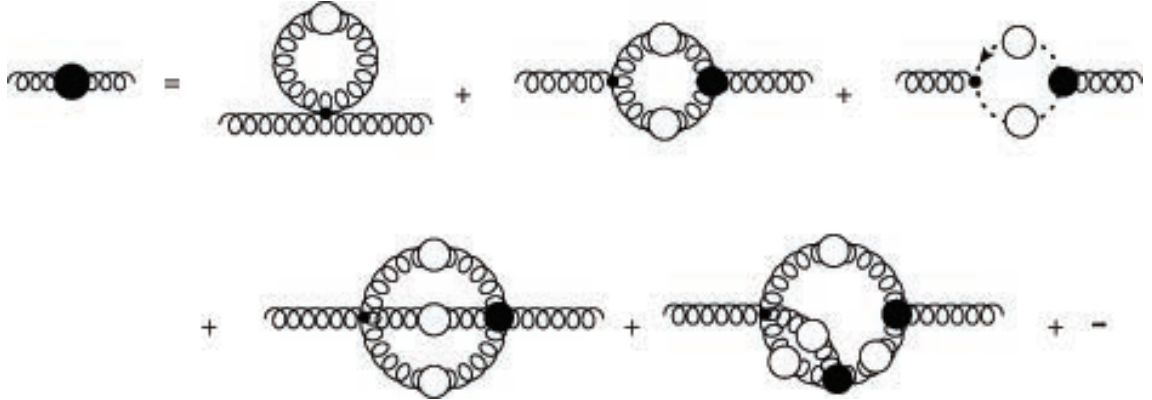


Figure 2.5: The SDE for the gluon propagator, showing some two dressed-loop contributions.

Therefore, the gluon propagator depends on all propagators and vertices of the theory, each of which satisfies its own SDE. The ghost-gluon vertex depends also on further correlation functions, such as the 4-point vertex in the last diagram of Fig.2.6.



Figure 2.6: SDE for the ghost-gluon vertex, up to 1 dressed-loop.

So, the SDEs constitute an infinite set of equations that intrinsically couple all correlation functions of the theory: They express the fact that there is no independent correlation function in QFT.

In principle, the SDEs concern full, i.e. all-order correlation functions. However, they may still miss some information, related to the vacuum of the theory or to topological effects [26]. Besides that, it is clear that the whole set of SDEs is intractable in practice: rigorously, solving exactly one SDE of a theory amounts to solving exactly all of them. Therefore, unless some kind of convergent limiting procedure is known, truncation is unavoidable in order to reduce the set of equations to a finite one.

Nevertheless, there is a history of researches improving self-consistent truncations that can yield solutions that would reveal the complete behavior of the theory. This will be discussed in Sect.3.2.

On the conceptual significance of SDEs, we note that, if the interactions are ultimately related to the correlation functions, the way quarks interact with each other, for instance, is intrinsically related to the behavior of *all* fields of the theory. This means that QFT holds a whole distinct picture of interactions: it does not speak of interactions *between* systems, but *among* them, and the impact of this feature depends on how relevant the quantum fluctuations can become in a theory.

Since the interactions are expected to be, in one way or another, responsible for confinement, this complex dynamics *might* be precisely what could enrich QCD in such a way that it would present all properties required for a theory to describe strong phenomena, from scaling (v. Sect.3.1) to confinement.

## 2.2 Renormalization

Such distinguished behaviors as the ones just mentioned bear an important feature of QFTs: the possibility that, in the same theory, the same degrees of freedom display strikingly different behaviors – from almost free at high resolution (i.e. high energies, or short distances), to strongly interacting at lower energies. This comes from renormalization, which can be introduced as the following.

Basically, a physical observable  $U$  is, on the theoretical side, given by a formal series in the parameters  $\{g_i\}$  of the theory <sup>§</sup>:

$$U(g_1, \dots, g_N) = \sum_{n=0}^{\infty} \sum_{i_1, \dots, i_n=1}^N U_{i_1, \dots, i_n} g_{i_1} \cdots g_{i_n} , \quad (2.22)$$

which, on the experimental side, is measured in terms of physical quantities such as scattering angles and energy, for example. Let us generally call (with a tendentious notation for particle physicists) these physical quantities  $s$ ,  $t$ , and  $u$ . Therefore,

$$U_{\text{exp}}(s, t, u)$$

is to be related to  $U(g_1, \dots, g_N)$ , so one already expects that the parameters of the theory should be functions of experimentally accessible physical variables. Taking  $N = 1$  for simplicity, a QFT should, then, lead to results like

$$U(g) = \sum_{n=0}^{\infty} U^{(n)} g^n =: f(g) \equiv f(g(s, t, u)) .$$

However, how could the theoretical parameters depend on such  $s$ ,  $t$ ,  $u$ , since no Lagrangian has any dependence on them to begin with? The answer comes from a further development of QFT: basically, it is renormalization, and the renormalization group (RG) that allow not only the relation from the Lagrangian parameters  $g$  to the measurable  $g(s, t, u)$ , but also relating their values in different conditions,  $g(s, t, u) \leftrightarrow g(s', t', u')$ .

In the next subsections we will give an overview of how this happens and its application to QCD. For more introductory details, we refer to [22], and for more specifics to [24, 27, 28, 21].

---

<sup>§</sup>Such as masses and couplings, but to be generally called as couplings (as one can rather think of masses as 2-point self-couplings).



### 2.2.1 Renormalized Lagrangians

We go back to the factor  $Z$  in the matrix elements (2.1) and (2.3), and note that it can be incorporated into the Green functions of the theory: Renormalizing the source  $J(x) \mapsto Z^{1/2}J(x)$ , or, equivalently, the field  $\varphi(x) \mapsto Z^{-1/2}\varphi(x)$ <sup>¶</sup>, leads to the renormalized correlation functions:

$$G_R^{(n)} = Z^{-n/2}G^{(n)} , \quad (2.23a)$$

$$G_{cR}^{(n)} = Z^{-n/2}G_c^{(n)} , \quad (2.23b)$$

$$\Gamma_R^{(n)} = Z^{n/2}\Gamma^{(n)} . \quad (2.23c)$$

These Green functions are functional derivatives of the renormalized Lagrangian, which is obtained by the above field renormalization, as well as by redefinition of any parameters present in the original Lagrangian. To exemplify it, we consider the scalar  $\varphi^4$  theory, with the Lagrangian

$$\mathcal{L} = \frac{1}{2} (\partial_\mu \varphi_0) (\partial^\mu \varphi_0) - \frac{1}{2} m_0^2 \varphi_0^2 - g_0 \varphi_0^4 .$$

Writing it as a function of the renormalized field and parameters, we obtain:

$$\begin{aligned} \mathcal{L} &= \frac{1}{2} Z (\partial_\mu \varphi) (\partial^\mu \varphi) - \frac{1}{2} m_0^2 Z \varphi^2 - g_0 Z^2 \varphi^4 \\ &= \frac{1}{2} (\partial_\mu \varphi) (\partial^\mu \varphi) - \frac{1}{2} m^2 \varphi^2 - g \varphi^4 + \mathcal{L}_c , \end{aligned}$$

where

$$\mathcal{L}_c = \frac{1}{2} (Z - 1) (\partial_\mu \varphi) (\partial^\mu \varphi) - \frac{1}{2} \delta_m \varphi^2 - \delta_g \varphi^4 ,$$

with  $\delta_m = m_0^2 Z - m^2$  and  $\delta_g = g_0 Z^2 - g$ .

Therefore, following this procedure, the renormalized theory is described by a Lagrangian just like the original one, having added  $\mathcal{L}_c$ , whose terms are called the counterterms, and can be treated as additional interactions of the theory.

The renormalized Lagrangian for QCD is:

$$\begin{aligned} \mathcal{L} &= -\frac{1}{4} Z_A (\partial_\mu A_\nu^a - \partial_\nu A_\mu^a) (\partial^\mu A^{a\nu} - \partial^\nu A^{a\mu}) + \frac{1}{2\xi} (\partial \cdot A^a) (\partial \cdot A^a) + \tilde{Z}_c (\partial^\mu \bar{c}^a) (\partial_\mu c^a) \\ &\quad + Z_F \bar{\psi}^j (i \not{\partial} - Z_{m_j} m_j) \psi^j - \tilde{Z}_1 g f^{abc} (\partial^\mu \bar{c}^a) c^b A_\mu^c + Z_{1F} g \bar{\psi}^j T_{jk}^a A^a \psi^k \\ &\quad - Z_3 \frac{g}{2} f^{abc} (\partial_\mu A_\nu^a - \partial_\nu A_\mu^a) A^{b\mu} A^{c\nu} - Z_4 \frac{g^2}{4} f^{abc} f^{cde} A_\mu^a A_\nu^b A^{c\mu} A^{d\nu} . \end{aligned} \quad (2.24)$$

---

<sup>¶</sup>That is, the renormalized field equals  $Z^{-1/2}$ ×the original one, which we denote then by  $\varphi_0$ .

## 2.2.2 Renormalization Group

The counterterms can be calculated order by order in perturbation, as depicted in Subsect.2.1.2: to each order in the coupling  $g$ , the counterterms are added to the loop contributions so as to cancel possible ultraviolet (UV) divergences that arise in the loop calculations [28, 25].

The UV divergences are parametrized within a certain regularization procedure, and the definition of the counterterms leads to their dependence on this regularization parameter. Each precise choice of counterterms amounts to a choice of renormalization scheme and scale. That is, the counterterms end up incorporating the UV divergences and, irrespective of the chosen scheme, through the regularization parameter they inevitably depend on some mass scale  $\mu$  [24, 27].

In this way, the definition of the counterterms is doubly arbitrary: by choosing one or another scheme, or by varying  $\mu$ , one obtains equally valid correlation functions to a given perturbative order (i.e. to a given power of  $g$ , or number of loops). To be more precise, let us take a proper vertex (2.23c): In momentum space, the unrenormalized vertex is a function of  $p$  and, say, of the coupling  $g$  and mass  $m$ . The renormalized vertex will be, then, also a function of  $\mu$ :

$$\Gamma_R^{(n)}(p, g, m, \mu) = Z^{n/2}(\mu)\Gamma^{(n)}(p, g, m) .$$

Then, the tautology  $d\Gamma^{(n)}/d\mu = 0$  proves itself very useful:

$$\implies \frac{d}{d\mu} \left\{ Z^{-n/2}(\mu)\Gamma_R^{(n)}(p, g, m, \mu) \right\} = 0 , \quad (2.25)$$

which in turn implies that:

$$\left( \mu \frac{\partial}{\partial \mu} + \beta \frac{\partial}{\partial g} - \gamma_m m \frac{\partial}{\partial m} - n\gamma \right) \Gamma_R^{(n)}(p, g, m, \mu) = 0 , \quad (2.26)$$

where

$$\beta \equiv \beta(g, m/\mu) = \mu \frac{\partial g}{\partial \mu} , \quad (2.27a)$$

$$\gamma_m \equiv \gamma(g, m/\mu) = -\frac{\mu}{m} \frac{\partial m}{\partial \mu} , \quad (2.27b)$$

$$\gamma \equiv \gamma(g, m/\mu) = \frac{\mu}{2Z} \frac{\partial Z}{\partial \mu} . \quad (2.27c)$$

So, the fact that the renormalized theory does come from the same Lagrangian, i.e. it is univocally determined despite the arbitrariness of its parameters, implies that these are actually constrained, satisfying equations (2.26) and (2.27) above. These are the renormalization group equations (RGEs).

For a given theory, the dependence of its RGEs on the mass scale  $\mu$  can be traded by the dependence on a momentum scale  $t$ , so that one ends up with total derivatives defining the RG functions, like e.g. for the  $\beta$  function:

$$\beta(g) = \frac{dg}{dt} ,$$

so that the  $\beta$  function describes the coupling  $g$  as a quantity depending on  $t$ , analogously to a phase space flow parametrized by  $t$  and given by  $\beta(g(t))$ . This flow accounts for the behavior of the interactions of the given theory with the momentum scale.

It was proven [29, 30] that QCD<sup>||</sup> presents a fixed point – which is a point  $(g_c, \beta(g_c)) \equiv (g_c, 0)$  – at  $g_c = 0$  in the UV. This behavior is called asymptotic freedom, and corresponds to a decreasing  $g$  that goes to zero as the momentum scale goes to infinity, so that the higher the energy, the weaker the interaction among the degrees of freedom of the theory.

It is unknown, however, whether or not QCD presents an IR fixed point, corresponding to  $\beta \rightarrow 0$  as  $g \rightarrow g'_c$  in the IR limit. As we shall describe next, while asymptotic freedom does allow a perturbative expansion in powers of the small coupling  $g$ , this method is only reliable in the UV, and nonperturbative approaches yet did not provide definite conclusions on the IR behavior of the strong coupling  $\alpha_s := g^2/4\pi$ .

---

<sup>||</sup>In fact any non-Abelian YM theory, with possible addition of up to (in the  $SU(3)$  case) 16 fermions.

## Chapter 3

# Quantum Chromodynamics

### 3.1 Perturbative QCD

#### 3.1.1 From valence quarks to distribution functions

Since Rutherford's atomic model [2], scattering experiments led to increasingly deeper access to the structure of matter, and it was not different for the substructure of hadrons.

In particular, deep inelastic scattering (DIS) experiments, in which a hadron-hadron, or a lepton-hadron scattering produces a final state with distinct particle content, were the ones to probe the hadrons' internal structure. Considering a lepton-hadron DIS, the cross-section has the form

$$\sigma_{\text{DIS}} \sim \sigma_0 [W_2 \cos^2(\theta/2) + 2W_1 \sin^2(\theta/2)] ,$$

where  $\theta$  is a certain scattering angle of the outgoing lepton,  $W_1$  and  $W_2$  are structure functions that carry the unknown details of the process, and  $\sigma_0$  is the cross-section for the collision between the incoming lepton and a charged particle.

It was seen [31] that the high-energy behavior of the structure functions corresponded to the hadron as being a collection of point-like particles – that is, when probed at higher resolutions, the hadron structure is seen as made of point-like constituents, which are Feynman's partons.

As experiments explored this internal structure, it became clear that those partons would not simply be the hadron's constituents as in the quark model (as the ones of Figs.1.1,1.2), but that there would be more – the called sea quarks. So, the understanding of e.g. a baryon evolved from the picture of three valence quarks, in Fig.3.1, to a picture of the valence quarks together with the sea quarks, as in Fig.3.2, to finally one with the full partonic constitution of quarks and gluons, Fig.3.3:

The distributions in the figures above are called the parton distribution functions (PDFs), which are a particular case of distribution functions for the structure of

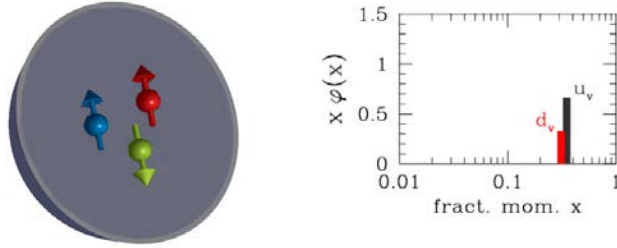


Figure 3.1: Representation of the proton as containing three valence quarks  $uud$ . On the right, the corresponding density distribution of these quarks with uniformly distributed fractions of the baryon's momentum.

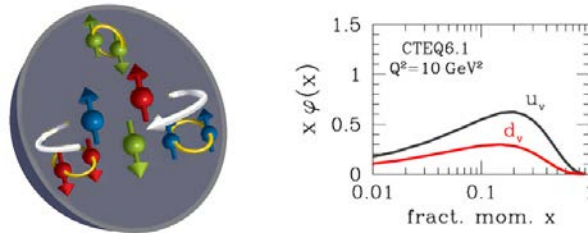


Figure 3.2: Representation of the proton as constituted by valence and sea quarks. On the right, now a continuous distribution of these quarks with respect to the fraction of the proton's momentum.

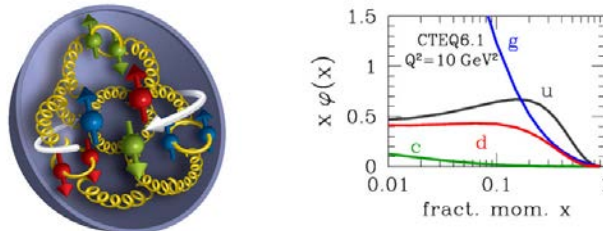


Figure 3.3: Representation of the full partonic picture of the proton, with a distribution of additional types of quarks and also gluons according to the graph shown on the right.

hadrons – there are others types and generalizations of parton distributions [32], all of them contributing to the understanding of this substructure, its dynamics, and the emergence of certain properties of hadrons. The understanding of hadrons' spins, for instance, is still an open problem, as well as the distinguished behavior of the gluon PDF, in contrast with the quarks', shown on the right in Fig.3.3.

Furthermore, the concept of PDFs allowed for one essential ingredient for perturbative QCD: factorization [33]. Generally put, it states that, in a hadron( $H_1$ )-

hadron( $H_2$ ) collision, the cross-section will be at least approximately given by

$$d\sigma_{H_1 H_2} \approx \sum_{ij \text{ types of partons}} \int_0^1 dx_1 \int_0^1 dx_2 f_{i/H_1}(x_1) f_{j/H_2}(x_2) d\hat{\sigma}_{ij}(x_1, x_2), \quad (3.1)$$

where  $f_{k,H}(x_k)$  is the density distribution of the parton  $k$  in the hadron  $H$  at momentum fraction  $x_k$ , and  $\hat{\sigma}_{ij}(x_1, x_2)$  is the partonic cross-section for the  $i$ - $j$  scattering, which can, then, be calculated within QCD.

### 3.1.2 Limitations of perturbative QCD

Asymptotic freedom enables such calculations to be done perturbatively, to increasing order in the coupling  $\alpha_s$ . The evolution from leading (LO) and next-to-leading order (NLO) towards next-to-next-to leading order (NNLO) and so on took quite some time to be accomplished.

The QCD beta function, for example, was determined to LO and NLO in the early 1970's, and to NNLO around six years later. Then almost two decades later it was computed to N<sup>3</sup>LO [34], a calculation that involved  $\mathcal{O}(10^4)$  diagrams.

The number of diagrams grows factorially with the number of loops, as well as with the number of legs, implying increasing complexity for calculations to higher orders, and convergence issues [28]. In fact, the perturbative series is only asymptotic: not necessarily convergent [35]. That is, it may not converge when higher order terms are added – even for small values of the coupling, due to the factorial growth with more loops.

Moreover, it is well-known that the coupling given by perturbation theory develops the so-called Landau pole – the divergence of  $\alpha_s(Q^2)$  at some scale  $Q \sim \Lambda_{QCD}$  – which is estimated [1] to be of the order of a few hundreds of  $MeV$ . Fig.3.4 shows the current experimental status of  $\alpha_s$ .

So, the  $\Lambda_{QCD}$  scale sets a boundary for the validity of the perturbative method – for energies smaller than this, it is definitely inadequate. The Landau singularity spoils the analyticity of the theory, introducing into physical amplitudes singularities that are not consistent with the behavior expected from analyticity conditions, on the theoretical side, and also from experiment.

So, perturbative QCD can evaluate  $\hat{\sigma}$  in Fig.3.5 below, which describes the various aspects and treatments involved in theoretically predicting experimental results in colliders. The PDFs for the colliding hadrons are experimentally determined, while the whole process after the parton scattering, in which highly energetic partons fragment into further ones until they end up hadronizing and forming jets, is greatly model-dependent [36].

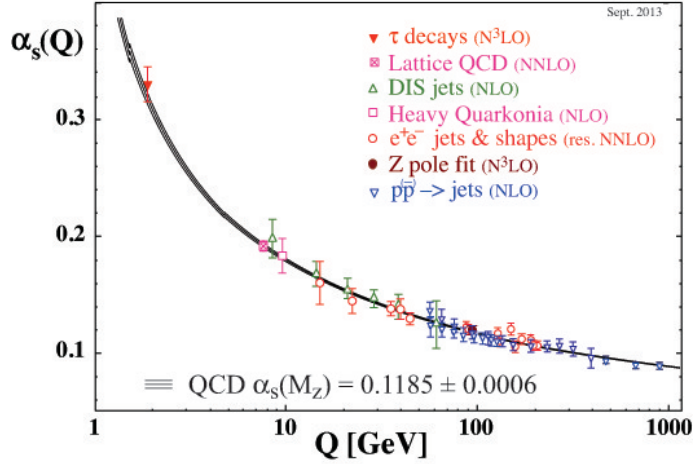


Figure 3.4: Summary of measurements of  $\alpha_s(Q^2)$ . Figure from [1].

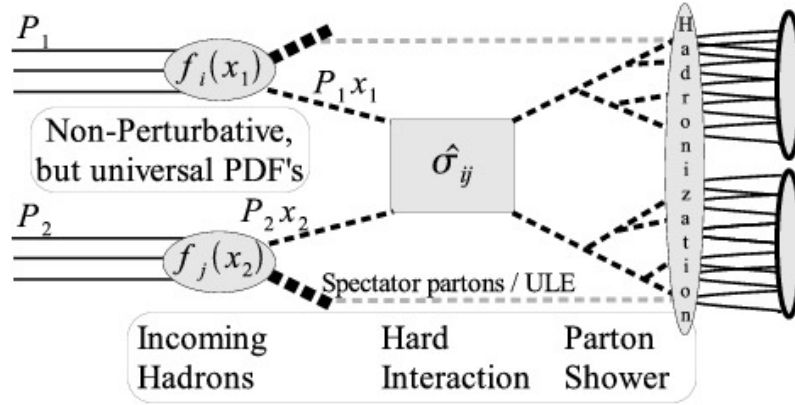


Figure 3.5: Concise depiction of the general theoretical treatment of hadron-hadron collisions. Credits for the figure: Ref.[37].)

So, the complexity of accelerator experiments is such that their analysis depend on complex tools such as algorithms for jet definition and event generators, as well as on fragmentation and hadronization models, which are also objects of current research and development.

### 3.2 Nonperturbative QCD

To believe that asymptotic freedom and the ever-increasing of  $\alpha_s$  make QCD's confinement understood is, *to some extent*, like believing that the transition from quantum to classical physics is understood from the verification of the classical limit of the path integral as  $\hbar \rightarrow 0$ . First, it is inaccurate to assert that  $\alpha_s$  indefinitely increases in the IR: this would be the behavior *if* perturbation theory were valid at

lower energies, which is not the case. Secondly, like there are approaches to describe decoherence as a process somehow brought about from QM, the understanding of *how* confinement takes place, somehow resulting from the many-particle character of a QFT when under the circumstances of the IR domain of QCD, is one ultimate goal of nonperturbative QCD researches.

The nonperturbative (NP) domain is marked by further characteristics besides confinement, e.g. vortices and topological effects [26], chiral symmetry breaking [38] and nontrivial condensates [39], whose relation among each other are also object of investigation, as well as how would they relate to the theory's correlation functions [40, 26].

There are in fact various approaches to these matters, from improved quantization [41, 42] and effective field theories [43], to lattice and SDEs, for instance. Among these (rather incomplete) mentions, we will focus on the latter, yet citing also lattice results, given that collaboration between lattice and continuum methods has been, in the past decade, source for corroborating conclusions in NP QCD.

### 3.2.1 Lattice and Schwinger-Dyson agreements

Along the years of QCD being well-established, some confinement scenarios were formulated, stating some or other – sometimes conflicting – properties of QCD, some of which concerning Green functions, as conditions for confinement to take place.

In particular, there were two types of behavior for the gluon and ghost propagators: one, of the called the scaling solutions, consists in a vanishing gluon propagator at zero momentum accompanied by an IR enhanced (i.e. more divergent than the tree-level  $1/p^2$ ) ghost one. Some SDE results for the gluon propagator [44, 45], for example, indicated an IR behavior  $\sim 1/(p^2)^2$ . This specific IR enhancement can be related [46, 18] to a linearly rising potential, accounting for a Schrödinger-like description of a bound state of (heavy) quarks, and satisfies the Wilson area law, which serves as a criterion for confinement [47].

The other kind is the behavior of the massive, or decoupling solutions [11, 48, 46, 50, 51], which give a (nonzero) finite freezing value for the gluon propagator, and the ghost one diverging as  $1/p^2$  in the deep IR – in other words, an also finite and nonzero ghost dressing.

While analytical approaches led to conclusions agreeing with either one or another scenario, it was the lattice computations [40] that strengthened the agreement in favor of the massive (decoupling) solutions, at least for  $SU(2)$  and  $SU(3)$  YM in



$D = 3$  and  $D = 4$ , and in the Landau gauge [49].\* This agreement is illustrated in Fig.3.6 below [50], which contrasts results from lattice and SDEs for the gluon propagator, and also its perturbative behavior.

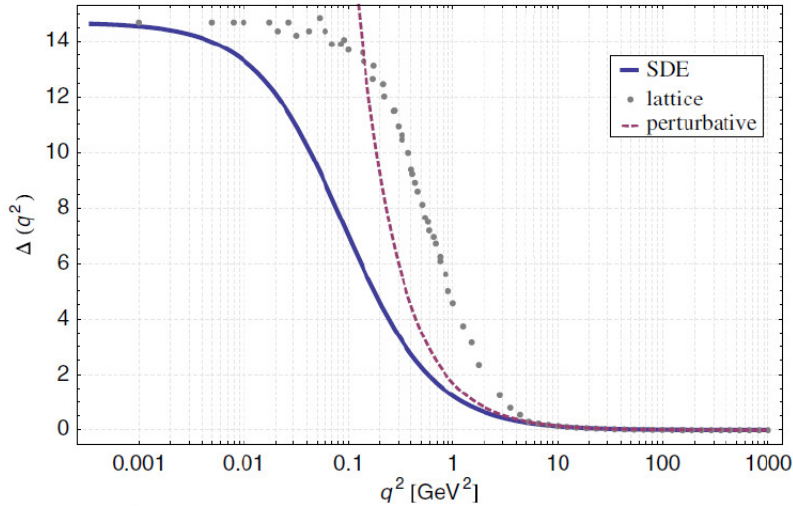


Figure 3.6: Comparison between SDE result from [50] and lattice result from [52], also contrasted with the perturbative (1-loop) behavior, showing the agreement on the massive-like solutions for the gluon. Credits for the Figure: Ref.[50].

### 3.2.2 Gluon mass and the strong coupling

Agreements such as the one displayed in Fig.3.6 contributed for the current general acceptance of massive gluons.

It is important to say, however, that this dynamical mass does not mean that there is a massive on-shell condition for the gluons – if there is any sense at all to speak of an on-shell condition for the QCD fields. The massive solution consists in a low-energy suppression that can be taken into account by a massive-like behavior as:

$$\Delta(p^2) \sim \frac{1}{p^2 + m_g^2(p^2)}, \quad (3.2)$$

where  $p$  is Euclidean and  $m_g$  is intrinsically momentum-dependent: it decreases monotonically with energy, going to zero [53] in the ultraviolet (UV) *and* assumes a finite value as energy decreases.

While the massive character of gluons has gained increasing acceptance, the

---

\*We are in the present work mainly concerned with the Landau gauge. There are, nevertheless, results for other gauges that may be of future interest.

status of the strong coupling is quite unresolved, since distinct approaches do not present enough agreement.

In fact, the very nonperturbative definition of  $\alpha_s$  is problematic: even though the Slavnov-Taylor identities<sup>†</sup> (STIs) [54, 24, 20, 55]

$$Z_g := \frac{\tilde{Z}_1}{\tilde{Z}_c Z_A^{1/2}} \equiv \frac{Z_{1F}}{Z_F Z_A^{1/2}} \equiv \frac{Z_3}{Z_A^{3/2}} \equiv \frac{Z_4^{1/2}}{Z_A}, \quad (3.3)$$

in principle provide an univocal definition, even nonperturbatively, their implementation in truncated SDEs can be nontrivial and they might as well be only approximately satisfied [56]. So, in practice, one should distinguish the nonperturbative coupling of each vertex by defining it in terms of either vertex  $\tilde{Z}_1$ ,  $Z_{1F}$ ,  $Z_3$ , or  $Z_4$  [56], and there is no guarantee in principle, due to the truncations and approximations involved, that the result would be the same had one chosen another vertex.

Nevertheless, there are some indications for an IR finite  $\alpha_s$ , coming from lattice and SDEs [57], as well as from phenomenological and from formal considerations [58, 11].

There is a particular proposal which is of our special interest: In one of the first suggestions of massive gluons [11], Cornwall also proposed an ansatz for the running coupling given by

$$\alpha(p^2) = \frac{1}{4\pi b \log \left[ \frac{(4m_g^2(p^2) + p^2)}{\Lambda_{\text{QCD}}^2} \right]}, \quad (3.4)$$

where  $m_g$  is the gauge-invariant dynamical gluon mass,  $b = (33 - 2n_f)/48\pi^2$ , and  $n_f$  is the number of fermions. This charge has been employed in phenomenological applications [13], and is consistent with a framework of SDEs, also introduced in [11], that yield massive gluon solutions – namely, the Pinch Technique.

### 3.2.3 Pinch Technique

The Pinch Technique (PT) is an operational framework that, by means of rearranging Feynman graphs, accomplishes the definition of new, gauge-invariant correlation functions, in the sense that they satisfy the Ward Identities (WIs) coming from the classical action of the theory.

Besides being simpler than the STIs, many of the WIs are linear in the proper vertices (inverse propagators included), which is one source of rearrangements characteristic of the PT: given some momentum in a diagram, a WI involving it can

---

<sup>†</sup>They are functional differential equations for  $\mathcal{Z}$ ,  $\mathcal{W}$ , and  $\Gamma$  implied by BRST invariance of the quantized theory, and that imply, in turn, identities for and among correlation functions of the theory.

cancel certain terms, or generate inverse propagators<sup>‡</sup> that will transform this diagram into another one which contains effective vertices that were not present in the Lagrangian in the first place [55].

This was just one example of how cancellations and rearrangements occur. More generally, the PT is a diagrammatic construction that implements, at the level of Green functions, properties that are typically displayed by physical observables<sup>§</sup>.

Further development of this technique established a more refined formulation [59, 55], leading to all-order results and allowing for a consistent PT framework of SDEs.

Usually, the (unavoidable) truncation scheme of a SDE system can spoil the cancellations that would occur if the whole sum were made and thus potentially breaks the gauge (or BRST) symmetry, as already mentioned on the STIs and the definition of the QCD charge. Therefore, the formulation of PT SDEs with gauge-independent building blocks stands as a great advance: since the SDEs are self-consistent by construction, they will provide, then, gauge invariant solutions as well [55].

The PT gluon propagator is then kept transverse to all orders, being given by

$$\Delta_{\mu\nu}(p^2) = \frac{1}{p^2 + m_g^2(p^2)} \perp_{\mu\nu(p)} (+0 \parallel_{\mu\nu(p)}) , \quad (3.5)$$

where

$$\perp_{\mu\nu(p)} := \delta_{\mu\nu} - \frac{p_\mu p_\nu}{p^2} , \quad (3.6a)$$

$$\parallel_{\mu\nu(p)} := \frac{p_\mu p_\nu}{p^2} , \quad (3.6b)$$

and  $p$  is Euclidean.

That is, in the PT framework a mass generation is allowed with no change in tensor structure of the gluon, nor violation of fundamental identities and constraints of the theory – a result that is also supported by lattice QCD ones [50]. Such dynamical mass generation in the usual, covariant gauges is a current object of research, and there are still problems with maintaining transversality and with violations of STIs [56].

The relation between the PT gluon propagator and the usual one is explored in [60], and they are equal to leading order in the dressed loop expansion (i.e. in the number of loops in the PT gluon SDE).

---

<sup>‡</sup>One can think of the WI in Eq.4.9 as a prototype.

<sup>§</sup>In fact, the PT effective correlation functions present further properties associated with physical quantities, and can be used as ingredients in a then reformulated perturbative expansion – not only for QCD, but also applied to Electroweak Theory (with symmetry breaking) [55].

## Connection with the Background Field Method

While the PT consists in a diagrammatic, operational procedure whose general and all-order formulation took some time to be established, before that a connection with the Background Field Method (BFM) was explored.

Basically, the BFM [61] is a quantization framework which decomposes the quantum field  $\varphi$  into a sum with a background one,  $\hat{\phi}$ . Making  $\varphi \mapsto \varphi + \hat{\phi}$  in (2.4a), one obtains the new generating function<sup>¶</sup>

$$\tilde{\mathcal{Z}}[J, \hat{\phi}] = \int \mathcal{D}\varphi \exp i \left( S[\varphi + \hat{\phi}] + J \cdot \varphi \right) ,$$

and correspondingly defines  $\tilde{\mathcal{W}}[J, \hat{\phi}]$ ,  $\tilde{\phi} = \delta\tilde{\mathcal{W}}/\delta J$  and  $\tilde{\Gamma}[\tilde{\phi}, \hat{\phi}]$ , which is promptly verified to satisfy

$$\tilde{\Gamma}[0, \hat{\phi}] = \Gamma[\phi]|_{\phi=\hat{\phi}} .$$

This means that the original effective action corresponds to the 1PI vacuum graphs in the presence of the background field  $\hat{\phi}$ .

Applying the BFM to a non-Abelian gauge theory, and properly extending the gauge symmetry to the background gluon field [61] defines what is called the background field gauge (BFG), whose Feynman rules contain both quantum and background gluons in external lines (but only quantum ones inside loops).

The key point is that the BFG correlation functions, just like the PT ones, satisfy WIs instead of STIs [55]. This observation led to the formulation of a correspondence between the PT and the Feynman BFG [62]. Later on, this correspondence was established for general BFGs, by generalizing the PT [63]. Although this generalized PT does not display all the PT features (such as analyticity and unitarity properties [55]), the gauge-invariance given by the WIs remains satisfied.

So, in this way, the PT-BFM connection allows computing (generalized) PT Green functions, which do satisfy WIs, by means of the usual QFT framework of BFG Feynman rules, which is potentially useful for our proposal of implementing NP properties into the usual Feynman rules language.

---

<sup>¶</sup>Note that the integration over dynamic variables is still  $\mathcal{D}\varphi$  only, since  $\hat{\phi}$  is a background, non-quantum field.

### 3.3 Improvements of the perturbative series

Returning to the open gap between QCD and hadronic physics, and to the aforementioned limitations of perturbative QCD, many authors consider that this problem could be overcome by reorganizing the perturbative series, and such procedure seems to depend on the strong coupling's behavior in the infrared (IR) [58].

One approach to this matter is the Analytical Perturbation Theory (APT) [64], in which an analyticity condition is imposed so that the Landau pole is systematically subtracted, order by order, and as a result the theory develops an IR fixed point. Nevertheless, some singularities remained, for example in Pomeron and Odderon models [65], resulting from the IR singularity of the gluon propagator.

So, while there are indications that an IR fixed point should be accompanied by a dynamical mass generation for the gluon [66], massive gluons had in fact been introduced *ad hoc* within the APT framework [67], whose phenomenological applications were shown to lead to a better convergence of the perturbative series [68].

Yet another approach to improve the perturbative series is the Dynamical Perturbation Theory (DPT) [10]. In this scheme, the quantities that are nonzero to every order in perturbation are given by their free field values, while quantities that decrease as  $\lambda \propto e^{-1/g^2}$  are kept to be possibly treated as expansions in  $g^n \lambda$ .

The DPT proposal lacked, though, account that typically non-Abelian diagrams in QCD disable an explicit separation between contributions from propagators and from vertices. This problem was discussed in later works [69] that postulated a skeleton expansion to 1-loop for QCD in which, for quark-quark scattering for example, the non-Abelian terms are decomposed [70] into two parts, each contributing either to vertices or to the gluon propagator.

The work [10] concerned mainly a dynamical mass generation for quarks. With the increasing agreement between lattice's and Schwinger-Dyson equations' (SDE) results on the gluon propagator, and with the indications that the coupling would be IR finite, we have motivation to extend the DPT idea considering these two effects also.

This effort began to be dealt with by applying Cornwall's effective charge (3.4) to phenomenological calculations at tree-level, together with a gluon mass of the form [51]:

$$m_g^2(Q^2) = \frac{m^4}{Q^2 + m^2} , \quad (3.7)$$

as a DPT-like approach to incorporate nonperturbative features into QCD processes described perturbatively.

In general [71], as shown in [13], various applications involving very different energy scales had fit reasonably well the experiments, and they all lead to the following range for the gluon mass at  $q^2 = 0$ :

$$m_0 \approx \mathcal{O}(1.2 - 2)\Lambda_{\text{QCD}} , \Lambda_{\text{QCD}} \approx 300\text{MeV} . \quad (3.8)$$

These tree-level applications have motivated a loop-level implementation of such nonperturbative features, leading to the work of the present thesis.

# Chapter 4

## Effective loop expansion

### 4.1 The proposal

Like DPT, our proposal is a pragmatic one for the development, even with no sound derivation yet, of a set of rules that could improve and extend perturbative QCD.

The desired method would provide, already at 1 loop, good results in the UV *and* deeper into the IR domain, consisting then in an effective-loop expansion not only extending the domain of validity of perturbation theory, but with faster convergence. That is, faster approach to the usual NNLO, N<sup>3</sup>LO and so on, incorporating, at 1 effective-loop, higher order and possibly intrinsic nonperturbative effects.

The first calculations within this scheme are to concern pure YM. In particular, this thesis presents the work with the ghost and the gluon propagators. Further applications to the ghost-gluon and the three-gluon vertices are in progress [15], to be followed by the inclusion of quarks, upgrading the proposed method from YM to QCD.

#### 4.1.1 First attempts and issues found

The first, simplest attempt concerned the Landau gauge ghost and gluon propagators, as well as the ghost-gluon vertex at zero gluon momentum. It is described in [14], and firstly involved dressing the gluon propagators inside loops, and nothing else.

We verified, though, that introducing only massive gluons as IR ingredient was not sufficient to successfully fit the lattice results for the three Green functions considered then. We explored fits varying parameters within an effective charge as well as with a constant  $\alpha_s$ . Although reasonably good fits, with the same set of values of fitting parameters for the three Green functions, were accomplished, we considered this first approach unsatisfactory for the following reasons. Besides

having employed an ad-hoc renormalization to cancel the divergences\*, by caution we ought to ponder whether the successful fitting could be due to an excessive number of parameters in the expression for the charge [14].

Moreover, the gluon self-energy then obtained was not transverse: dressing gluons in the loops generates a nontrivial longitudinal component even in the Landau gauge, definitely violating BRST symmetry and the STIs. As there are no such violations in the PT-BFM framework, we then proceeded to explore it. This is detailed in Sect.4.3.

Meanwhile, we built a basic code with symbolic calculations in the software *Mathematica*, using the *FeynCalc* package for some manipulations.

Later on, we built our own code, directly and exclusively with *Mathematica* language, properly designed for our proposal and therefore more efficient for our purposes. This routine is described in Appendix A, and allowed us to explore the problem of transversality of the gluon self-energy, to work with general  $R_\xi$  gauges and to futurely compute further correlation functions in general momentum configurations.

#### 4.1.2 Methodology

The procedure is: first, assume certain forms of the quantities (propagators, vertices) present in each 1-loop expansion: some dressed, some not, composing the “1-effective-loop” expansion that can be viewed as an approximation of the corresponding SDE.

As to be detailed in the next section, our expansion dresses the gluon propagator and the background-quantum-quantum gluon vertex, while the ghost dressing and the ghost-gluon vertex are set to their tree-level forms, since researches indicate [72] they display nonperturbative behavior qualitatively similar to their respective perturbative one.

After calculated, this 1-effective-loop correction is analyzed according with certain renormalization schemes, described in Sect.4.4, to be compared with available lattice results, which presumably correspond to all orders in conventional perturbation expansion.

This comparison is to tell, then, if such effective-1-loop expansion is a good approximation to what would be a higher order result, for correlation functions at least, and in this sense being a better convergent expansion, able to access deeper into the IR domain of the theory.

---

\*What we consider to be ad-hoc or not will be detailed in Sect.4.4. In particular, the schemes employed in this first attempt were the ones given by (4.17) and (4.18).



This project aims to make calculations analytically, with symbolic computations only, yet in *Mathematica*. The reason for an analytical treatment is twofold. On one hand, there already are very powerful numerical approaches concerning nonperturbative YM and QCD, such as lattice, SDEs and Bethe-Salpeter equations. On the other hand, and more importantly for practical purposes: for the desired method to be applicable to QCD phenomenology, it had better be simple at the level of the loop calculations themselves, since the perturbative machinery from there to actual testable predictions is very complicated already, as pointed out in Chap.3.

So, a method that is analytically computable at the level of Feynman diagrams can stand more chances to be useful in the whole picture of perturbative QCD, and then to provide a link between the UV and IR domains.

In the following sections, we detail the approximations, procedures for calculations, and further considerations for developing the desired effective-loop expansion.

## 4.2 Gluon and ghost propagators to 1 effective-loop

From the SDE for the gluon self-energy (Fig.2.5), we have:

$$\Sigma_{\mu\nu}^{ab}(p) = -\delta^{ab} N g^2 \frac{1}{\mu^{D-4}} \int \frac{d^D l}{(2\pi)^D} \left\{ \frac{1}{2} \Gamma_{\mu\rho\tau(p,-l,l-p)} \Gamma_{\nu\sigma\alpha(-p,l,p-l)} \Delta_{(l)}^{\rho\sigma} \Delta_{(p-l)}^{\tau\alpha} \right. \quad (4.1a)$$

$$\left. + \frac{1}{2} [2g_{\mu\nu} g_{\rho\tau} - (1-y)(g_{\mu\rho} g_{\nu\tau} + g_{\mu\tau} g_{\nu\rho})] \Delta_{(l)}^{\rho\tau} \right. \quad (4.1b)$$

$$\left. + \tilde{\Gamma}_{\mu(l-p,p,-l)} \tilde{\Gamma}_{\nu(l,-p,p-l)} \frac{F_{(l)} F_{(p-l)}}{l^2 (p-l)^2} - 2\beta g_{\mu\nu} \frac{F_{(l)}}{l^2} \right\} , \quad (4.1c)$$

where the parameters  $y$  and  $\beta$  distinguish the cases considered – the background gluon in the BFG, or the quantum gluon in the  $R_\xi$  covariant gauges (CG), respectively given by:

$$\begin{cases} \beta = 1 & \& y = 1/\xi, \text{ for BFG} \\ \beta = 0 & \& y = 0, \text{ for CG} \end{cases} , \quad (4.2)$$

and:  $\Gamma$  is the bare three-gluon (or background-quantum-quantum gluon in the BFG),  $\mathbf{\Gamma}$  is the dressed one;  $\tilde{\Gamma}$  is the bare ghost-gluon vertex,  $\tilde{\mathbf{\Gamma}}$  the dressed one;  $\mathbf{\Delta}$  is the full gluon propagator, and  $F$  is the ghost dressing.

Our present approximation considers:

$$\tilde{\mathbf{\Gamma}}_{\mu(k_2,q,-k_1)} = \tilde{\Gamma}_{\mu(k_2,q,-k_1)} , \quad (4.3a)$$

$$F_{(k)} = 1 , \quad (4.3b)$$

$$\mathbf{\Gamma}_{\alpha\mu\nu(q,p_1,p_2)} = \Gamma_{\alpha\mu\nu(q,p_1,p_2)} + V_{\alpha\mu\nu(q,p_1,p_2)} . \quad (4.3c)$$

The dressing of  $\Gamma$ , in (4.3c), will be discussed in the next section. For the dressed gluon propagator inside loops, we take

$$\Delta_{\mu\nu(k)} = \frac{1}{k^2 + m^2} \perp_{\mu\nu(k)} + \frac{\xi}{k^2} \parallel_{\mu\nu(k)} . \quad (4.4)$$

Representing these approximations diagrammatically, the gluon self-energy that we calculate is given in Fig.4.1:

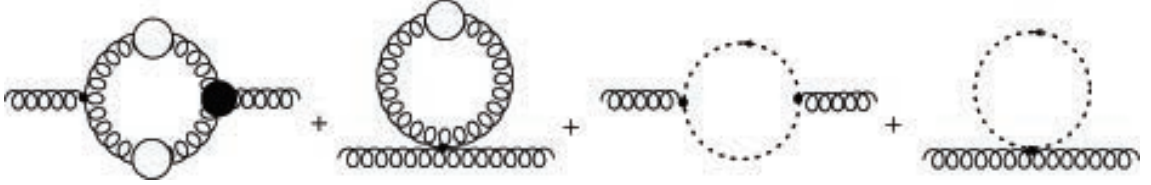


Figure 4.1: Diagrams contributing to the gluon self-energy in this approach. Each diagram depends on the parametrization (4.2) specifying whether the external gluon is a background or a quantum one.

The constant mass  $m$  in (4.4) is an approximation to the dynamical, running mass  $m(k^2)$  discussed in the previous chapter. In particular, if we compare the transverse part  $1/(k^2 + m_g^2)$  with

$$m_g^2 \equiv m^2(k^2) = \frac{m^4}{m^2 + k^2} \quad (4.5)$$

and with  $m_g^2 \equiv m^2(0) := m$ , we see that this is a reasonable approximation, as Fig.4.2 below shows.

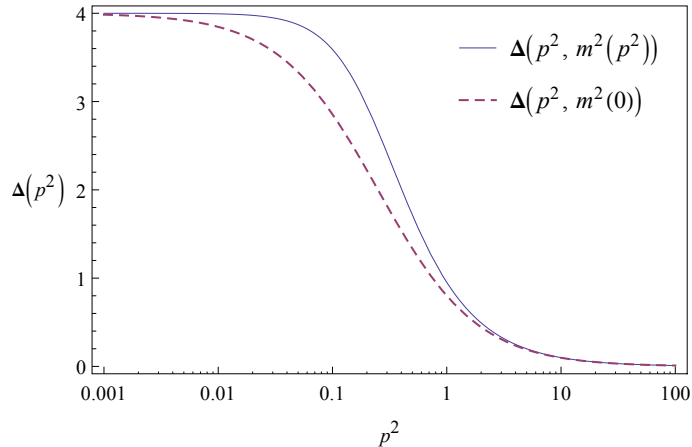


Figure 4.2: Comparison of the transverse part of (4.4) with the dynamical mass (4.5), and with a constant mass  $m := m^2(0)$ , taken to be  $500 MeV$  for this graph, while  $p^2$  is in  $GeV^2$  units.

In other words, we employ the approximation

$$\Delta_{\mu\nu}(k^2, m^2(k^2)) \approx \Delta_{\mu\nu}(k^2, m^2(0)) . \quad (4.6)$$

The same approximations for the ghost self-energy amount to the diagram in Fig.4.3 below.

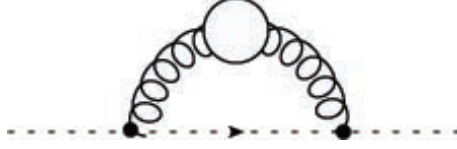


Figure 4.3: Diagram corresponding to the ghost self-energy. There is no dependence on the parameters in (4.2), since the gluons inside loops are always quantum ones.

### 4.3 Transversality of the gluon propagator

One desired feature for the effective loop expansion is that does not generate longitudinal corrections for the gluon propagator – i.e. that the incorporation of non-perturbative properties must only affect its transverse component.

The transverse and the longitudinal components of the self-energy are respectively given by:

$$\begin{aligned} \Sigma_{\perp} &= \frac{1}{(D-1)} \perp_{(p)}^{\mu\nu} \Sigma_{\mu\nu}(p) , \\ \Sigma_{\parallel} &= \parallel_{(p)}^{\mu\nu} \Sigma_{\mu\nu}(p) , \end{aligned}$$

where  $\Sigma_{\mu\nu}^{ab}(p) =: \Sigma_{\mu\nu}(p) \delta^{ab}$ . So let us consider each contribution that constitutes  $\Sigma_{\parallel}$ . The ghost sector contribution (4.1c) is readily evaluated to be

$$\parallel_{(p)}^{\mu\nu} \int d^D l \left( \tilde{\Gamma}_{\mu(l-p, p, -l)} \tilde{\Gamma}_{\nu(l, -p, p-l)} \frac{1}{l^2 (p-l)^2} - 2\beta g_{\mu\nu} \frac{1}{l^2} \right) = \frac{1}{4} (1-\beta)^2 \int d^D l \frac{1}{l^2} \left( 2 - \frac{p^2}{(p-l)^2} \right) .$$

As expected from the PT-BFM correspondence [55], the ghost sector is transverse in the BFG ( $\beta = 1$ ), irrespective of the specific gauge  $\xi$ . For the covariant gauges ( $\beta = 0$ ), the above contribution is to be summed up with the other ones.

For the tadpole diagram:

$$\parallel_{(p)}^{\mu\nu} \left( \frac{1}{2} [2g_{\mu\nu} g_{\rho\tau} - (1-y)(g_{\mu\rho} g_{\nu\tau} + g_{\mu\tau} g_{\nu\rho})] \Delta_{(l)}^{\rho\tau} \right) = \frac{1}{p^2} \left[ \Delta_{\rho\sigma(p)}^{-1} + \left( y - \frac{1}{\xi} \right) p_{\rho} p_{\sigma} \right] \Delta_{(l)}^{\rho\sigma} ,$$

and finally we proceed to the contribution (4.1a):

$$\parallel_{(p)}^{\mu\nu} \left( \frac{1}{2} \Gamma_{\mu\rho\tau(p, -l, l-p)} \Gamma_{\nu\sigma\alpha(-p, l, p-l)} \Delta_{(l)}^{\rho\sigma} \Delta_{(p-l)}^{\tau\alpha} \right) ,$$

and started exploring the hint, from the WI [60] within the BFM, that the transversality of the gluon self-energy might be achieved with some dressing for the three-gluon vertex in our 1 loop expansion.

At the beginning, we investigated a general  $V$  for the dressing (4.3c) and tried to constrain it by imposing the vanishing of the longitudinal component of the gluon self-energy. However, we recognized that, for being too general, it was not a good strategy to start with, so we added the assumption that the function  $V$  would be given by the ansatz considered in [73, 12], which is a function of the PT (or BFM) gluon self-energy and, for our approximation (4.6), becomes

$$V_{\alpha\mu\nu(p,p_1,p_2)} = \frac{\Theta_{\alpha\mu\rho(p,p_1)}}{p^2 p_1^2} \perp_{(p_2)}^{\rho\nu} + \text{cyc. perm.} , \quad (4.7)$$

where

$$\Theta_{\alpha\mu\rho(k,q)} = \theta \frac{m^2}{2} k^\alpha q^\mu (k - q)_\rho , \quad (4.8)$$

and with  $\theta = 1$ . We kept, however,  $\theta$  in the calculations as a parametrization of the dressing of this vertex, so we can analyze the effects of employing or not this ansatz.

We then verified that the gluon self-energy is transverse with this vertex, for  $\theta = 1$ , and for *any* BFG. In fact, the vertex in this case does satisfy the referred WI

$$p^\alpha \left( \Gamma_{\alpha\mu\nu(p,p_1,p_2)} + V_{\alpha\mu\nu(p,p_1,p_2)} \right) \Big|_{p=-p_1-p_2} = \Delta_{\mu\nu(p_1)}^{-1} - \Delta_{\mu\nu(p_2)}^{-1} . \quad (4.9)$$

Given this positive result, we proceeded to compute the ghost and gluon propagators, whose results must be renormalized since, as expected from analytical loop calculations, divergences will be generated in the formalism.

## 4.4 Renormalization

From (2.18a), we have for the gluon propagator in terms of the Euclidean momentum  $p$ :

$$\begin{aligned} G_{\mu\nu}^{ab-1}(p) &= i \left\{ -\Gamma_{\mu\nu}^{ab(0)}(p) - i\delta^{ab} \frac{N\alpha_s}{16\pi} \Pi_{\mu\nu}(p) \right\} , \\ \implies G_{\mu\nu}^{-1}(p) &= - \left( G_{\mu\nu}^{(0)} \right)^{-1}(p) + \frac{N\alpha_s}{16\pi} \Pi_{\mu\nu}(p) . \end{aligned}$$

Taking the transverse part, we have:

$$G^{-1}(p) = p^2 + \frac{N\alpha_s}{16\pi} \Pi(p) , \quad (4.10)$$

which can be renormalized according to two approaches: we can follow the renormalized perturbation theory (RPT) by adding counterterms, or else the renormalization

procedure employed for SDEs and the lattice [49] – which we shall call nonperturbative renormalization (NPR). Given that the effective expansion proposed is a hybrid between the usual perturbation and the SDEs, that would connect the IR and UV domains, it is not clear in principle which renormalization paradigm should be followed – or whether an also hybrid renormalization should be constructed.

So, we have analyzed three approaches, to be detailed in the following subsections. For the general expression (4.10), the NPR approach amounts to making

$$G^{-1}(p) \mapsto G_R^{-1}(p, \mu) = Z(\mu^2) \left[ p^2 + \frac{N}{16\pi} \alpha_s \Pi(p) \right], \quad (4.11)$$

while following RPT, on the other hand, we have

$$\begin{aligned} G^{-1}(p) &= p^2 + \frac{N}{16\pi} \alpha_s \Pi(p) - \Gamma_{\text{counterterms}}^{AA} \\ &= p^2 + \frac{N}{16\pi} \alpha_s \Pi(p) + p^2 \delta_Z + m^2 \delta_m, \end{aligned} \quad (4.12)$$

where it will be necessary to introduce, in addition to  $\delta_Z$ , also a mass counterterm  $\delta_m$ .

This is a potentially controverse point, due to the idea that a renormalizable theory should only have counterterms of the form of terms already present in the Lagrangian, so that  $\delta_m$  would only make sense had we considered a tree-level gluon mass. However, the dynamical gluon mass is of intrinsically nonperturbative character, coming from a dynamics that no finite order in (usual) perturbation can describe. Our proposal intends to preserve it that way: it consists in a method, as opposed to a model. While keeping the YM Lagrangian unchanged, we dress some quantities inside loops in order to introduce the whole behavior of the theory *into the fluctuations*.

While within SDE approaches no renormalization factor is necessary for the gluon mass generation, our proposal is expected to touch this matter because it implements intrinsic nonperturbative properties *into the usual formalism of loops*, which traditionally contained only tree-level ingredients.

Moreover, the  $m^2$  divergence is a direct consequence of our approximation, in the loop integral, of the dynamical mass  $m^2(p^2)$  to its freezing value  $m^2(0)$ . So, had we not made this approximation, there would be no massive UV divergence, since  $m^2(p^2 \rightarrow \infty) \rightarrow 0$ .

Finally, the above renormalizability paradigm can be extended [21, 24] to the possible addition of a *finite* number of counterterms, besides the ones of Lagrangian form.

According to this, we could add the counterterm  $\delta_m$  as long as it would suffice at more effective-loops. Their implementation may, though, not even make sense in our approach: Since we expect the 1 effective-loop Green function to account for its whole all-order, nonperturbative behavior, e.g. by fitting lattice results, consequently the very proposal of effective loop expansion is to suffice at 1 effective-loop.

Given these observations, our proposal seems compatible with the renormalizability paradigm in its extended form, and the addition of  $\delta_m$  is justified for renormalizing our results following the standards of RPT.

Proceeding with the analysis, we consider the general form of our results for the propagators, which is:

$$\Pi(p) = p^2 [(A + Bs^{-1}) \bar{\gamma} + f(s)] , \quad (4.13)$$

where

$$\bar{\gamma} := \frac{2}{D-4} + \gamma + \log\left(\frac{m^2}{4\pi\nu^2}\right) , \quad (4.14)$$

$A$  and  $B$  are constants,  $f(s)$  is a function of  $s := p^2/m^2$ , and  $p$  is the Euclidean momentum. For the ghost,  $B \equiv 0$ , while for the gluon we have one result for the BFG and another for the transverse part in the CG, shown in Sect. 5.1. With (4.13), (4.11) and (4.12) become:

$$G_R^{-1}(p, \mu) = Z(\mu^2) \left\{ p^2 \left( 1 + \frac{N}{16\pi} \alpha_s [(A + Bs^{-1}) \bar{\gamma} + f(s)] \right) \right\} , \quad (4.15)$$

$$G^{-1}(p) = p^2 \left\{ 1 + \frac{N}{16\pi} \alpha_s [(A + Bs^{-1}) \bar{\gamma} + f(s)] + \delta_Z \right\} + m^2 \delta_m , \quad (4.16)$$

which we consider in detail, then.

#### 4.4.1 Nonperturbative renormalization

Evidently, only one renormalization condition will not cancel both  $p^2$  and  $m^2$  divergences. Therefore, within this approach alone an ad-hoc scheme is unavoidable. From (4.15), we obtain:

$$G_R^{-1}(p, \mu) = G_R^{-1}(\mu, \mu) \frac{p^2 \left( 1 + \frac{N}{16\pi} \alpha_s [(A + Bs^{-1}) \bar{\gamma} + f(s)] \right)}{\mu^2 \left( 1 + \frac{N}{16\pi} \alpha_s [(A + B\sigma^{-1}) \bar{\gamma} + f(\sigma)] \right)} ,$$

where  $\sigma := \mu^2/m^2$ . We can deal with this in two ways: implementing an ad-hoc  $\overline{MS}$ -like subtraction for both divergences, or expanding this fraction into a difference. The former would consist in annihilating the  $\bar{\gamma}$  terms, leading to:

$$G_R^{-1}(p, \mu) \mapsto G_R^{-1}(p, \mu) = G_R^{-1}(\mu, \mu) \frac{p^2 \left(1 + \frac{N}{16\pi} \alpha_s f(s)\right)}{\mu^2 \left(1 + \frac{N}{16\pi} \alpha_s f(\sigma)\right)}. \quad (4.17)$$

Now, the expansion in  $\alpha_s$  must be cautious. Since we will dress  $\alpha_s$  later on, i.e. implement its running with momentum, we should expand the expression for  $G_R^{-1}$ , whose denominator is a function of  $\mu$  instead of  $p$ , so the expansion will correspond to one around the value  $\alpha_s(\mu) = 0$ , thus being consistent even after dressing the coupling. Doing that, we obtain

$$G_R^{-1}(p, \mu) = G_R^{-1}(\mu, \mu) \frac{p^2}{\mu^2} \left\{ 1 + \frac{N}{16\pi} \alpha_s [B (s^{-1} - \sigma^{-1}) \bar{\gamma} + f(s) - f(\sigma)] \right\},$$

so an additional ad-hoc condition must still be imposed in order to cancel the  $m^2$  divergence above. Opting again for  $\overline{MS}$ -like yields

$$G_R^{-1}(p, \mu) = G_R^{-1}(\mu, \mu) \frac{p^2}{\mu^2} \left\{ 1 + \frac{N}{16\pi} \alpha_s [f(s) - f(\sigma)] \right\}. \quad (4.18)$$

#### 4.4.2 Hybrid approach

Another way is to try a hybrid between the two renormalization paradigms: RPT for  $\delta_Z$ , and a multiplicative factor like in NPR, together with expansion in  $\alpha(\mu)$  to try canceling the  $m^2$  divergence.

Starting with

$$G^{-1}(p, \mu_1) = p^2 \left\{ 1 + \frac{N}{16\pi} \alpha_s [(A + B s^{-1}) \bar{\gamma} + f(s)] + \delta_Z(\mu_1) \right\},$$

we determine  $\delta_Z$  in terms of the value  $G^{-1}(\mu_1, \mu_1)$ , and then apply a NPR procedure

$$G_R^{-1}(p, \mu_1, \mu_2) = Z(\mu_2) G^{-1}(p, \mu_1), \quad (4.19)$$

with the multiplicative factor  $Z(\mu_2)$  given in terms of the value of  $G_R^{-1}(\mu_2, \mu_1, \mu_2)$ . Doing this, we obtain

$$\frac{G_R^{-1}(p, \mu_1, \mu_2)}{G_R^{-1}(\mu_2, \mu_1, \mu_2)} = \frac{p^2 \left\{ 1 + \frac{N}{16\pi} \alpha_s G(\mu_1, \mu_1) \mu_1^2 [B (s^{-1} - \sigma_1^{-1}) \bar{\gamma} + f(s) - f(\sigma_1)] \right\}}{\mu_2^2 \left\{ 1 + \frac{N}{16\pi} \alpha_s G(\mu_1, \mu_1) \mu_1^2 [B (\sigma_2^{-1} - \sigma_1^{-1}) \bar{\gamma} + f(\sigma_2) - f(\sigma_1)] \right\}},$$

which requires an  $\overline{MS}$ -like scheme to cancel the  $B$  terms, by making  $B \mapsto 0$ , whether we expand the above expression or not. We do this and remain considering both cases, as follows:

$$G_R^{-1}(p, \mu_1, \mu_2) = G_R^{-1}(\mu_2, \mu_1, \mu_2) \frac{p^2}{\mu_2^2} \left\{ 1 + \frac{N}{16\pi} \alpha_s G(\mu_1, \mu_1) \mu_1^2 [f(s) - f(\sigma_2)] \right\}, \quad (4.20)$$

and

$$G_R^{-1}(p, \mu_1, \mu_2) = G_R^{-1}(\mu_2, \mu_1, \mu_2) \frac{p^2}{\mu_2^2} \frac{1 + \frac{N}{16\pi} \alpha_s G(\mu_1, \mu_1) \mu_1^2 [f(s) - f(\sigma_1)]}{1 + \frac{N}{16\pi} \alpha_s G(\mu_1, \mu_1) \mu_1^2 [f(\sigma_2) - f(\sigma_1)]}. \quad (4.21)$$

The factor  $Z(\mu_2)$  in expression (4.19) can actually account for the multiplicative factor that is in principle arbitrary [74] in lattice computations of Green functions. That is, the NPR procedure of (4.19) corresponds to relating the 1 loop result  $G_{\text{loop}}$  to the lattice one,  $G_{\text{lattice}}$ :

$$G_{\text{lattice}}^{-1}(p) = Z(\mu_2) G_{\text{loop}}^{-1}(p, \mu_1), \quad (4.22)$$

thus accounting for the arbitrary overall constant in  $G_{\text{lattice}}$ . We will return to this point when analyzing the results obtained for the 1 effective-loops.

We note that for the ghost, the second scale  $\mu_2$  is unnecessary, so this scheme need not be considered for renormalization of the ghost propagator. Also, we emphasize the need for an ad-hoc cancellation of the mass divergence in all approaches until this point. As we will see, there is only one case in which we could give a more founded cancellation of divergences, and it was within RPT.

### 4.4.3 Renormalized Perturbation

We know that fixing the value of the full propagator at one momentum scale suffices to fix one counterterm. As we argued in the beginning of this section, it does make sense in our proposal to introduce a mass counterterm. In order to fix  $\delta_m$  within a momentum subtraction (MOM) scheme, we can choose a second momentum scale.

More precisely: with expression (4.16), we simultaneously fix the values  $G(\mu_1)$  and  $G(\mu_2)$ , and, with two linear equations, we can find consistent solutions writing  $\delta_Z$  and  $\delta_m$  in terms of them. This leads to the following equivalent expressions:

$$\begin{aligned} G^{-1}(p) &= G^{-1}(\mu_1) + \frac{N}{16\pi} \alpha_s [p^2 f(s) - \mu_1^2 f(\sigma_1)] \\ &+ \frac{(p^2 - \mu_1^2)}{(\mu_1^2 - \mu_2^2)} \left[ G^{-1}(\mu_1) - G^{-1}(\mu_2) - \frac{N}{16\pi} \alpha_s [\mu_1^2 f(\sigma_1) - \mu_2^2 f(\sigma_2)] \right] \end{aligned} \quad (4.23)$$

$$\begin{aligned} &= G^{-1}(\mu_2) + \frac{N}{16\pi} \alpha_s [p^2 f(s) - \mu_2^2 f(\sigma_2)] \\ &+ \frac{(p^2 - \mu_2^2)}{(\mu_1^2 - \mu_2^2)} \left[ G^{-1}(\mu_1) - G^{-1}(\mu_2) - \frac{N}{16\pi} \alpha_s [\mu_1^2 f(\sigma_1) - \mu_2^2 f(\sigma_2)] \right] \end{aligned} \quad (4.24)$$

In the next chapter, when renormalizing our results, we will choose one scale, say  $\mu_1$ , in the UV, and set  $G$  to its tree-level form

$$G(\mu_1^2) = \frac{1}{\mu_1^2}. \quad (4.25)$$



This will be enough for the ghost propagator. For the gluon, the need for another scale can actually be meaningful. Recalling the approximation of the dynamical mass  $m(p^2)$  to  $m(0)$ ,  $\mu_2$  can serve to make our result consistent with the mass we used in loops as the freezing value  $m(0) =: m$ : We can do this by choosing  $\mu_2$  in the IR, and setting

$$G(\mu_2^2) = \frac{1}{m^2 + \mu_2^2} . \quad (4.26)$$

For the ghost propagator, we have

$$\tilde{G}^{-1}(p) = p^2 \left\{ 1 + \frac{N}{16\pi} \alpha_s [A\bar{\gamma} + f(s)] + \delta_Z \right\} =: p^2 F^{-1}(p) , \quad (4.27)$$

where  $F(p)$  is the ghost dressing function. So, fixing  $\delta_Z$  in terms of the value  $F(\mu)$ , we obtain

$$F(p)^{-1} = F(\mu)^{-1} + \frac{N\alpha_s}{16\pi} [f(s) - f(\sigma)] , \quad (4.28)$$

which is the RPT expression for the ghost dressing function, in the MOM scheme. As in (4.25), we will set  $F(\mu) = 1$  for  $\mu$  in the UV.

Although (4.23) and (4.24) are more complicated expressions, they are the less arbitrary ones, since they require neither ad-hoc  $\overline{MS}$ -like vanishings  $A, B \mapsto 0$ . Moreover, given that our approach aims to link and access both UV and IR domains, the above setting of scales seems reasonable. Finally the IR condition relates the mass renormalization with the freezing of the gluon mass, which is the main ingredient of the effective loop expansion proposed. For these reasons, the RPT approach described above is, at least conceptually, the preferred one by us. It is in the next chapter, though, that the results will tell whether this renormalization scheme will turn out to be successful or not.

There are, nevertheless, further ingredients in our effective expansion.

## 4.5 Further dressings: effective charge and running mass

We advocated the dressing of the gluon propagator inside loops based on its distinguished IR behavior, given by the dynamical mass generation. Having evaluated the loop integrals, we obtain expressions in terms of  $\alpha_s$ , which also may display such distinguished behavior. As referred in Chap.3, an IR finite coupling may as well accompany an IR finite gluon propagator, besides indications of this behavior from nonperturbative methods. Considering that we want to describe both UV and IR domains, dressing  $\alpha_s \mapsto \alpha_s(p^2)$  is a compelling idea.

Since we also want to arrive at analytical expressions for our 1-effective loop Green functions, we maintain the ‘‘Cornwall-inspired’’ guidance and opt to employ his analytical expression (3.4)

$$\alpha_s(p^2) = \frac{4\pi}{11 \log [(4m^2(p^2) + p^2) / \Lambda_{\text{QCD}}^2]}, \quad (4.29)$$

where we shall take  $\Lambda_{\text{QCD}} = r m(0)$  and consider  $r \in [1, 3]$ , based on phenomenological approaches mentioned in Chap.3.

We note that the above expression contains the dynamical, running gluon mass, so we decided to explore the following two cases. One, with all dependence in  $m$  being the constant value  $\approx m(0)$ , and the other implementing its running. That is,

$$\alpha_s(p^2) = \frac{4\pi}{11 \log \left( \frac{r^2(4m_g^2 + p^2)}{m^2} \right)} \quad \text{and} \quad s = \frac{p^2}{m_g^2}, \quad (4.30)$$

where:

$$\text{either } m_g^2 \equiv m^2(0) =: m^2, \quad (4.31)$$

$$\text{or } m_g^2 \equiv m^2(p^2) = \frac{m^4}{m^2 + p^2}. \quad (4.32)$$

In other words, we will analyze both cases  $G(p^2, m^2(0))$  and  $G(p^2, m^2(p^2))$ . Now, the expressions of the previous section become, following the same order as before:

$$G_R^{-1}(p, \mu) = G_R^{-1}(\mu, \mu) \frac{p^2 \left( 1 + \frac{N}{16\pi} \alpha_s(p^2) f(s) \right)}{\mu^2 \left( 1 + \frac{N}{16\pi} \alpha_s(\mu^2) f(\sigma) \right)}, \quad (4.33)$$

$$G_R^{-1}(p, \mu) = G_R^{-1}(\mu, \mu) \frac{p^2}{\mu^2} \left( 1 + \frac{N}{16\pi} [\alpha_s(p^2) f(s) - \alpha_s(\mu^2) f(\sigma)] \right), \quad (4.34)$$

$$G_R^{-1}(p, \mu_1, \mu_2) = G_R^{-1}(\mu_2, \mu_1, \mu_2) \frac{p^2}{\mu_2^2} \left( 1 + \frac{N}{16\pi} G(\mu_1, \mu_1) \mu_1^2 [\alpha_s(p^2) f(s) - \alpha_s(\mu_2^2) f(\sigma_2)] \right), \quad (4.35)$$

$$G_R^{-1}(p, \mu_1, \mu_2) = G_R^{-1}(\mu_2, \mu_1, \mu_2) \frac{p^2}{\mu_2^2} \frac{1 + \frac{N}{16\pi} G(\mu_1, \mu_1) \mu_1^2 [\alpha_s(p^2) f(s) - \alpha_s(\mu_1^2) f(\sigma_1)]}{1 + \frac{N}{16\pi} G(\mu_1, \mu_1) \mu_1^2 [\alpha_s(\mu_2^2) f(\sigma_2) - \alpha_s(\mu_1^2) f(\sigma_1)]}, \quad (4.36)$$

$$\begin{aligned}
G^{-1}(p) &= G^{-1}(\mu_1) + \frac{N}{16\pi} [p^2 \alpha_s(p^2) f(s) - \mu_1^2 \alpha_s(\mu_1^2) f(\sigma_1)] \\
&+ \frac{(p^2 - \mu_1^2)}{(\mu_1^2 - \mu_2^2)} \left[ G^{-1}(\mu_1) - G^{-1}(\mu_2) - \frac{N}{16\pi} [\mu_1^2 \alpha_s(\mu_1^2) f(\sigma_1) - \mu_2^2 \alpha_s(\mu_2^2) f(\sigma_2)] \right] \quad (4.37) \\
&= G^{-1}(\mu_2) + \frac{N}{16\pi} [p^2 \alpha_s(p^2) f(s) - \mu_2^2 \alpha_s(\mu_2^2) f(\sigma_2)] \\
&+ \frac{(p^2 - \mu_2^2)}{(\mu_1^2 - \mu_2^2)} \left[ G^{-1}(\mu_1) - G^{-1}(\mu_2) - \frac{N}{16\pi} [\mu_1^2 \alpha_s(\mu_1^2) f(\sigma_1) - \mu_2^2 \alpha_s(\mu_2^2) f(\sigma_2)] \right] , \quad (4.38)
\end{aligned}$$

$$F(p)^{-1} = F(\mu)^{-1} + \frac{N}{16\pi} [\alpha_s(s) f(s) - \alpha_s(\sigma) f(\sigma)] . \quad (4.39)$$

With the definitions (4.30), (4.31), and (4.32), the above expressions were applied to the results for the ghost and the gluon self-energies, which we continue to present in the following chapter.

# Chapter 5

## Results

### 5.1 Analytical expressions

In this section we present some results obtained from the *Mathematica* code developed. Following the notation of the previous chapter for the self-energy  $\Pi$ , in this one we shall write  $\Pi \equiv p^2\zeta$ . That is, from (4.10),

$$G^{-1}(p) = p^2 \left( 1 + \frac{N\alpha_s}{16\pi} \zeta(p) \right) ,$$

and from (4.13), then:

$$\zeta(p) = (A + Bs^{-1}) \bar{\gamma} + f(s) \tag{5.1}$$

is the general form of the results to be shown next, directly relatable to the renormalized dressed expressions (4.33)-(4.38).

#### 5.1.1 Gluon propagator

The gluon self-energy is decomposed into transverse ( $\perp_{\mu\nu(p)}$ ) and longitudinal ( $\parallel_{\mu\nu(p)}$ ) terms, denoted respectively as  $\zeta_{\perp}$  and  $\zeta_{\parallel}$ . Also, superscripts BFG or CG will denote the results for the background field or covariant gauges, respectively.

In the BFG, the longitudinal part indeed vanishes for  $\theta = 1$ , while the best one could do in CG (at D=4) is to obtain a finite longitudinal term for  $\theta = (1 + \xi)/\xi$ . In this case, this finite part is

$$\zeta_{\parallel}^{CG} |_{\theta=(1+\xi)/\xi} = -\frac{4+s}{s^2} + \frac{(1+s)(4-s+s^2)}{s^3} \log(1+s) - \log(s) ,$$

so that, definitely, no dressing of the form (4.7,4.8) for the three-gluon vertex can render a vanishing longitudinal term for the (quantum) gluon self-energy. Nevertheless, this does not exclude the possibility that another form of dressing might accomplish that, so this remains then as an open problem.

For the BFG, the general result for the longitudinal part is:

$$\zeta_{\parallel}^{BFG}(p^2) = (\theta - 1) \left[ -\frac{3(\xi - 1)}{s} \bar{\gamma} + \frac{(-3\xi + (4\xi - 5)s - 1)}{s^2} - \log(s) + \frac{(1 + s)(3\xi + s^2 + (2 - 3\xi)s + 1)}{s^3} \log(1 + s) \right].$$

Therefore, the 1 effective-loop BFG self-energy is transverse, *irrespective of the gauge choice*: the dressing (4.7,4.8) for the background-gluon-gluon vertex, with  $\theta = 1$ , guarantees the **gauge-independent\* transversality of the background gluon self-energy**, as actually expected from the WI (4.9) satisfied by that dressed vertex.

Now, for the transverse part, it turns out that all its dependence on  $\theta$  is proportional to  $\xi^2$  and  $\xi^2 y$ , so that, *whether in the BFG or the CG, the transverse part is independent of  $\theta$  in the Landau gauge*.

The expression obtained for the BFG gluon self-energy is, for general  $\xi$  and  $\theta$ , and (below) also for the Landau gauge:

$$\begin{aligned} \zeta_{\perp}^{BFG} = & -\frac{(3(\theta - 3)\xi + 44s + 9)}{s} \bar{\gamma} \\ & + \frac{-3\xi + 3(\xi^2 + 7\xi + 15)s^2 + s(30\xi^2 + (4\theta + 6)\xi - 37) - 1}{s^2} \\ & + \frac{(-6\theta\xi + s^3 + (6\xi - 4)s^2 - 6(2\xi + 1)s)}{2s} \log(s) \\ & + \frac{(1 - s)(1 + s)(3\xi + s^3 + 3(\xi - 3)s^2 - 3(2\xi + 3)s + 1)}{s^3} \log(1 + s) \\ & - \frac{1}{2} (s^2 - 20s + 12) \left( \frac{s + 4}{s} \right)^{3/2} \log \left( \frac{\sqrt{s + 4} - \sqrt{s}}{\sqrt{s + 4} + \sqrt{s}} \right) \\ \xrightarrow{\xi=0} & - (44 + 9s^{-1}) \bar{\gamma} + 45 - 37s^{-1} - s^{-2} + \frac{1}{2} (s^2 - 4s - 6) \log(s) \\ & + \frac{(1 - s)(1 + s)^2 (s^2 - 10s + 1)}{s^3} \log(1 + s) \\ & - \frac{1}{2} (s^2 - 20s + 12) \left( \frac{s + 4}{s} \right)^{3/2} \log \left( \frac{\sqrt{s + 4} - \sqrt{s}}{\sqrt{s + 4} + \sqrt{s}} \right), \end{aligned} \quad (5.2)$$

---

\*That is, independent of the gauge choice  $\xi$ .

while the corresponding result for the CG case is

$$\begin{aligned}
\zeta_{\perp}^{CG} &= \frac{(9\xi + 6\xi s - 26s + 9)}{s} \bar{\gamma} + \frac{-3\xi + (3\xi^2 + 13\xi + 23)s^2 + 3s(\theta\xi^2 + 2\xi - 19) + 1}{s^2} \\
&\quad - \frac{(1+s)(-3\xi + s^4 + (3\xi - 8)s^3 - 9(\xi + 2)s^2 + (9\xi - 8)s + 1)}{s^3} \log(1+s) \\
&\quad + \frac{1}{2}(s^2 + 6\xi s - 2) \log(s) - \frac{1}{2}(s^2 - 20s + 12) \left(\frac{s+4}{s}\right)^{3/2} \log\left(\frac{\sqrt{s+4} - \sqrt{s}}{\sqrt{s+4} + \sqrt{s}}\right) \\
\stackrel{\xi=0}{\mapsto} &- (26 - 9s^{-1}) \bar{\gamma} + 23 - 57s^{-1} + s^{-2} - \frac{(1+s)^3(s^2 - 10s + 1)}{s^3} \log(1+s) \\
&\quad + \frac{1}{2}(s^2 - 2) \log(s) - \frac{1}{2}(s^2 - 20s + 12) \left(\frac{s+4}{s}\right)^{3/2} \log\left(\frac{\sqrt{s+4} - \sqrt{s}}{\sqrt{s+4} + \sqrt{s}}\right).
\end{aligned} \tag{5.3}$$

Also for general case and then in the Landau gauge, the CG longitudinal term obtained is:

$$\begin{aligned}
\zeta_{\parallel}^{CG} &= -\frac{3(\xi(\theta - 1) - 1)}{s} \bar{\gamma} + \frac{-3(\theta - 1)\xi + s(4(\theta - 1)\xi - 5) - 1}{s^2} \\
&\quad + \frac{(1+s)(3(\theta - 1)\xi + s^2 + s(2 - 3(\theta - 1)\xi) + 1)}{s^3} \log(1+s) - \log(s) \\
\stackrel{\xi=0}{\mapsto} &3s^{-1} \bar{\gamma} - \frac{5s + 1}{s^2} + \frac{(1+s)^3}{s^3} \log(1+s) - \log(s).
\end{aligned} \tag{5.4}$$

A comparison between this longitudinal and the corresponding transverse part can be given by the ratio  $\zeta_{\parallel}^{CG}/\zeta_{\perp}^{CG}$ . However, previous renormalization is necessary for this comparison, and there seems to be no preferred scheme for the longitudinal term: as opposed to the  $\delta_m$  case, we do not consider the introduction of a counterterm, say  $\delta_{\parallel}$ , a good procedure to be part of our proposal, given that such longitudinal term amounts to violation of symmetries in either BFG or CG case, and that dynamical gluon mass generation can be made compatible with a vanishing longitudinal self-energy. Yet, in order to do *some* comparison, we employed last chapter's  $\overline{MS}$ -like scheme, and considered the ratio

$$R_{MS'} := \frac{\zeta_{\parallel}^{CG}|_{A,B \rightarrow 0}}{\zeta_{\perp}^{CG}|_{A,B \rightarrow 0}}, \tag{5.5}$$

which is shown in Fig.5.1 below.

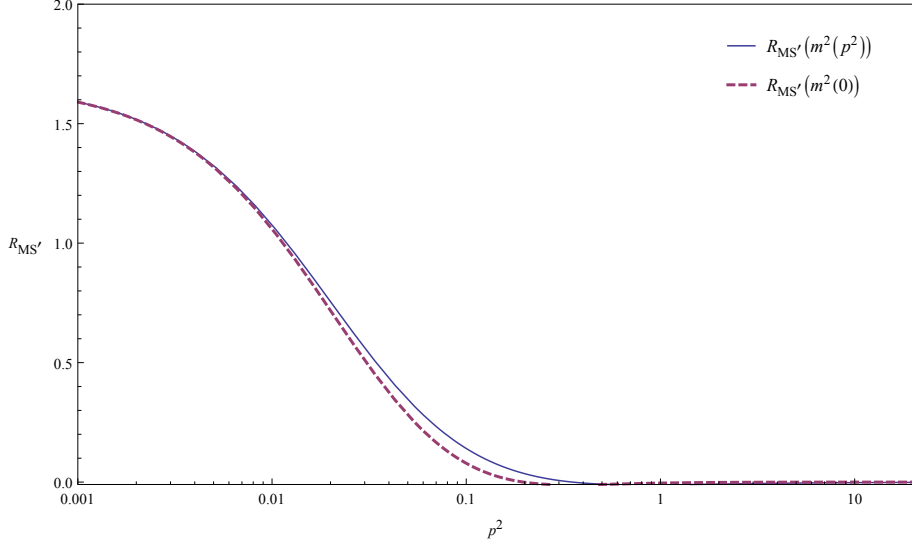


Figure 5.1: Ratio (5.5) between the longitudinal and the transverse CG self-energies, with divergences canceled by the  $\overline{MS}$ -like scheme. The  $p^2$  scale is  $GeV^2$  and  $m = 500MeV$ .

So, for  $p^2 \gtrsim 0.1GeV^2$ , the ( $\overline{MS}$ -like) longitudinal self-energy is definitely negligible compared to the transverse one. For lower energies, though, it develops the same order of magnitude,  $\zeta_{\parallel}^{CG}|_{A,B \rightarrow 0}$  being even greater than its transverse counterpart for  $p^2 \lesssim 0.01GeV^2$ .

While it is unknown how would this longitudinal-term generation affect further, phenomenological applications, this is definitely a problem for of the effective-loop proposal when applied to correlation functions, and it could not but be exposed. We remark, still, that this comparison is renormalization-scheme dependent, and anticipate the results of next section that this particular scheme did not provide good results for the gluon propagator, so conclusions drawn from it should be considered with care. In any case, the BFG already stands in advantage for providing a consistent framework for the desired effective-loop expansions.

### 5.1.2 Ghost propagator

The result obtained for the ghost self-energy is:

$$\begin{aligned} \tilde{\zeta} &= (3 - \xi)\bar{\gamma} - 5 - s^{-1} - (\xi + s) \log(s) + \frac{(1 + s)^3}{s^2} \log(1 + s) \\ \xrightarrow{\xi=0} & 3\bar{\gamma} - 5 - s^{-1} - s \log(s) + \frac{(1 + s)^3}{s^2} \log(1 + s) . \end{aligned} \quad (5.6)$$

## 5.2 Successful renormalization schemes

Among the results given above, the ones for the Landau gauge were analyzed according with each of the renormalization approaches and schemes presented in Sect.4.4.

The ghost dressing presented the same qualitative behavior for both NPR and RPT cases, yet with values of freezing not only different, but of different orders of magnitude: Expressions (4.33) and (4.34) led to freezing values  $F(p^2 \rightarrow 0) \sim 120$  (for  $m = 500MeV$ ,  $r = 2$ ), and a strong dependence on the renormalization scale  $\mu$ : going from  $\mu = 100GeV^2$  to  $1000GeV^2$ , the freezing goes from  $\sim 120$  to  $\sim 1200$ . On the other hand, the scheme (4.37),(4.38) led to a freezing value  $\sim 1.25$ , and to only slight variation with  $\mu^2$  from 100 to  $1000GeV^2$ . For  $F(\mu^2 = 100GeV^2) = 1$ , the result is shown in Fig.5.2:

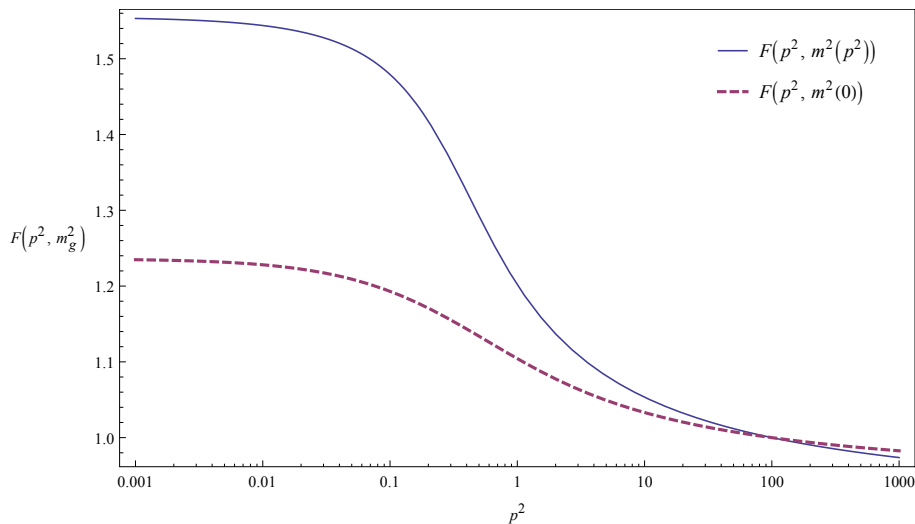


Figure 5.2: RPT-MOM (4.39) renormalized ghost dressing function, contrasted when dependent on a constant or a running gluon mass  $m_g$ . The squared momentum  $p^2$  is in  $GeV^2$  units,  $\mu = 100GeV^2$ ,  $m = 500MeV$ , and  $r = 2$ .

For the gluon propagator the situation was distinct. For both BFG and CG cases, the only successful approach in reaching the expected qualitative behavior was the RPT one.

This is actually a pleasant result because, first, it indicates a preferable renormalization approach and scheme; second, because, as explained in 4.4, the RPT given by (4.23), (4.24), (4.28) is the one we consider better founded.

The *qualitative* behavior agreeing with lattice and SDEs was obtained, within the RPT-MOM scheme, for the Landau gauge, with  $\mu_1^2 = \mu^2 = 100GeV^2$ , and, for the gluon case, with  $\mu_2^2 = 0.001GeV^2$  also. Figs.5.3,5.4 below present these succeeded



RPT-MOM renormalized gluon propagator results for both constant and dynamical gluon mass.

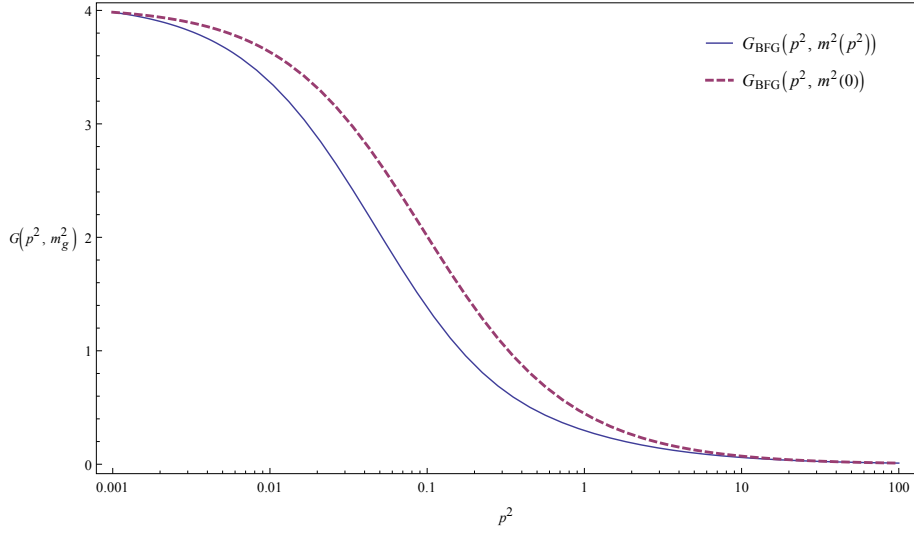


Figure 5.3: RPT-MOM (4.37) renormalized background gluon propagator, contrasted when dependent on a constant or a running gluon mass  $m_g$ . The squared momentum  $p^2$  is in  $GeV^2$  units,  $\mu = 100GeV^2$ ,  $m = 500MeV$ , and  $r = 2$ .

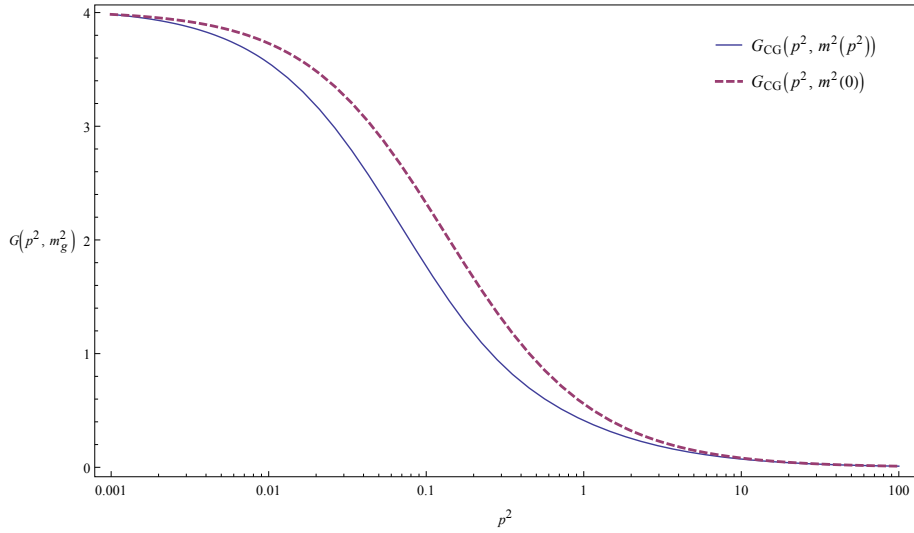


Figure 5.4: RPT-MOM (4.37) renormalized (transverse part of) quantum gluon propagator, contrasted when dependent on a constant or a running gluon mass  $m_g$ . The squared momentum  $p^2$  is in  $GeV^2$  units,  $\mu = 100GeV^2$ ,  $m = 500MeV$ , and  $r = 2$ .

The next graph compares directly the CG and the BFG results, for the case of a dynamical mass.

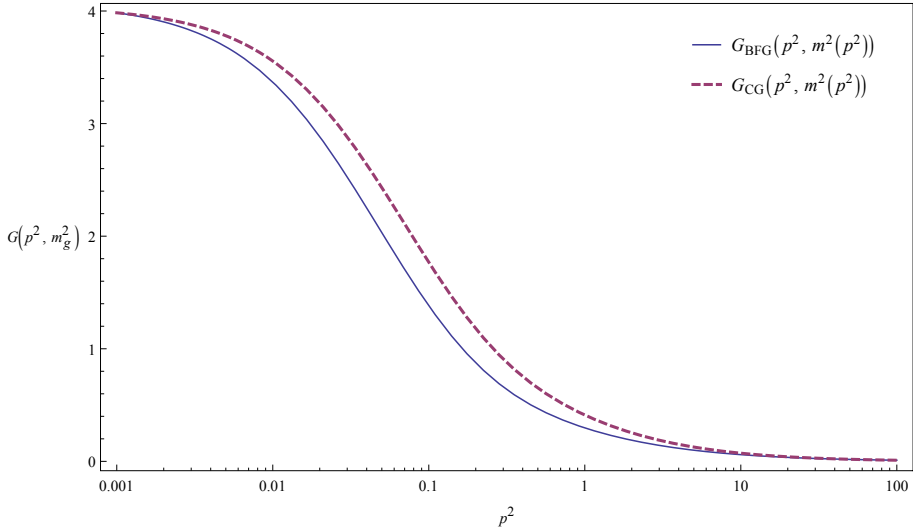


Figure 5.5: Comparison between the close RPT-MOM (4.37) results for the CG and BFG, for the case of a constant mass. Also,  $p^2$  is in  $GeV^2$  units,  $\mu = 100GeV^2$ ,  $m = 500MeV$ , and  $r = 2$ .

In fact, the RPT-MOM scheme was the only case for which the BFG and the transverse CG results were similar, as shown in Fig.5.5, which is potentially interesting from a practical point of view, as discarding the longitudinal term  $\zeta_{\parallel}^{CG}$  (i.e. keeping  $\zeta_{\perp}^{CG}$  only) yet would approximate the exactly transverse result  $\zeta^{BFG}$ .

Furthermore, we see a more significant difference between the employment of a constant or a dynamical mass for the ghost dressing  $F$ , giving distinct freezing values, 1.24 and 1.55 respectively.

The reason is not so much for this difference being present in  $F$ , but for it being absent in  $G$ . Since the RPT for the gluon involved an IR scale  $\mu_2$ , both  $G(m^2(0))$  and  $G(m^2(p^2))$  cases are constrained to a freezing value  $G(\mu_2)$  – in our renormalization choice, equal to  $1/(\mu_2^2 + m^2(0))$  and  $1/(\mu_2^2 + m^2(\mu_2^2))$  respectively. For the ghost propagator and dressing, there is no such constraint, therefore allowing manifest difference between the dynamical and the constant mass cases for  $F(p \rightarrow 0)$ . Nevertheless, we should note that those two freezing values do correspond to very

close curves for the ghost propagator, as shown in Fig.5.6 below.

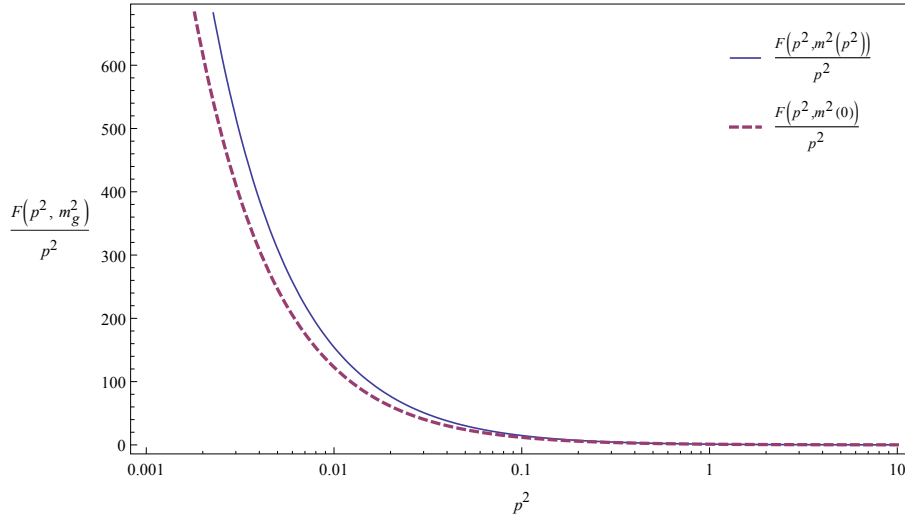


Figure 5.6: Curves for the ghost propagator corresponding to the dressing functions of Fig.5.2, for a constant or a running gluon mass  $m_g$ . Still,  $p^2$  is in  $GeV^2$  units,  $\mu = 100GeV^2$ ,  $m = 500MeV$ , and  $r = 2$ .

Moreover, the constraint on the freezing  $G(p^2 \rightarrow 0)$  of the gluon propagator to be given by the gluon mass recalls us of the consideration, expressed in (4.22), that lattice results for Green functions are given up to an arbitrary overall (multiplicative) factor.

Since our results should not lose their UV limit to the perturbative behavior, comparison with lattice data will likely require rescaling the latter by a multiplicative factor.

### 5.3 Comparison to lattice results

In this section, we will compare our effective-loop results to both lattice and the usual perturbative ones. The latter is taken from the massless limit of our results, which, from (5.1) within the RPT, are given by:

$$G^{-1}(p) = p^2 \left\{ 1 + \frac{N\alpha_s}{16\pi} \left( A \left[ \frac{2}{D-4} + \gamma + \log \left( \frac{p^2}{4\pi\nu^2} \right) \right] + f_0(p) \right) + \delta_Z \right\} ,$$

where  $f_0(p) = \lim_{m \rightarrow 0} [f(s) - A \log(s)]$ . Taking the MOM renormalization scheme yields

$$G^{-1}(p) = p^2 \left\{ \frac{G^{-1}(\mu)}{\mu^2} + \frac{N\alpha_s}{16\pi} \left[ A \log \left( \frac{p^2}{\mu^2} \right) + f_0(p) - f_0(\mu) \right] \right\} ,$$

where  $f_0$  are constants for all cases considered. Also, taking  $\alpha_s$  as Cornwall's charge (3.4) evaluated at the renormalization scale  $\mu$ , we have

$$G^{-1}(p) = p^2 \left\{ \frac{G^{-1}(\mu)}{\mu^2} + \frac{N}{16\pi} \alpha_s(\mu^2) A \log \left( \frac{p^2}{\mu^2} \right) \right\} \quad (5.7)$$

as the (usual, massless) perturbative expressions to be contrasted with our results.

The lattice results are from [75], and will be compared with ours for  $m = 500MeV$ ,  $r := m/\Lambda_{QCD} = 2$ , and  $\mu^2 = \mu_1^2 = 100GeV^2$ .

### 5.3.1 Gluon propagator

Since our approach for the gluon propagator included a consistency renormalization condition  $G(\mu_2) = 1/(m^2 + \mu_2^2)$  in the IR, the first rescaling of lattice data will be based on this IR condition.

The lowest value of momentum for which there is lattice data is precisely the  $\mu_2^2 = 0.001GeV^2$  that we considered in our general analysis of the previous section. Then, we divided the whole set of data by a common factor so that the lattice value at  $\mu_2$  would equal our  $G(\mu_2) = 1/(m^2 + \mu_2^2)$ , for  $m = 500MeV$  in this case<sup>†</sup>. The contrasts are shown in Figs.5.7,5.8 below.

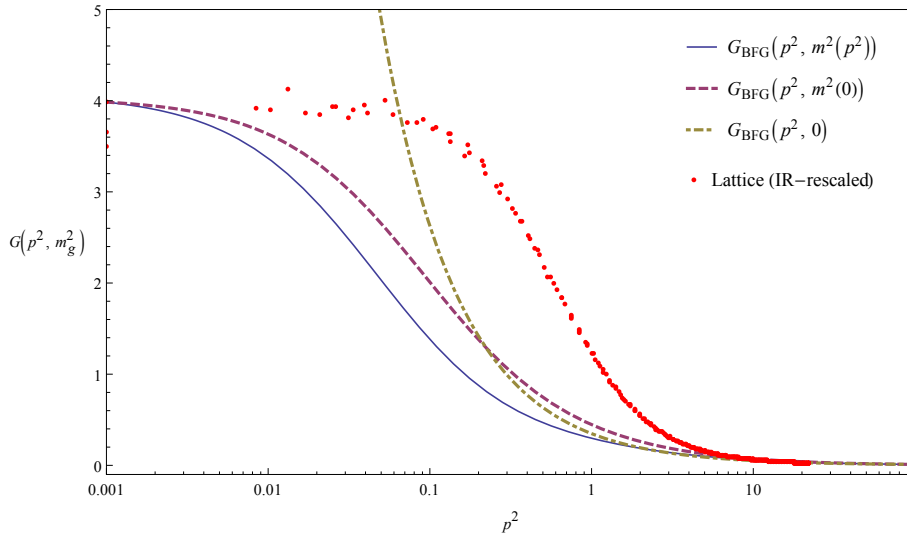


Figure 5.7: Comparison of our BFG results for the gluon propagator with dynamical and constant gluon mass to the (massless 1-loop) perturbative result, and to lattice data rescaled in the IR.  $p^2$  is in  $GeV^2$  units,  $\mu_1 = 100GeV^2$ ,  $m = 500MeV$ , and  $r = 2$ .

<sup>†</sup>Different combinations with  $m = 600MeV$  and  $r = 1.2$  were also considered, and lead to similar contrasts with the lattice.

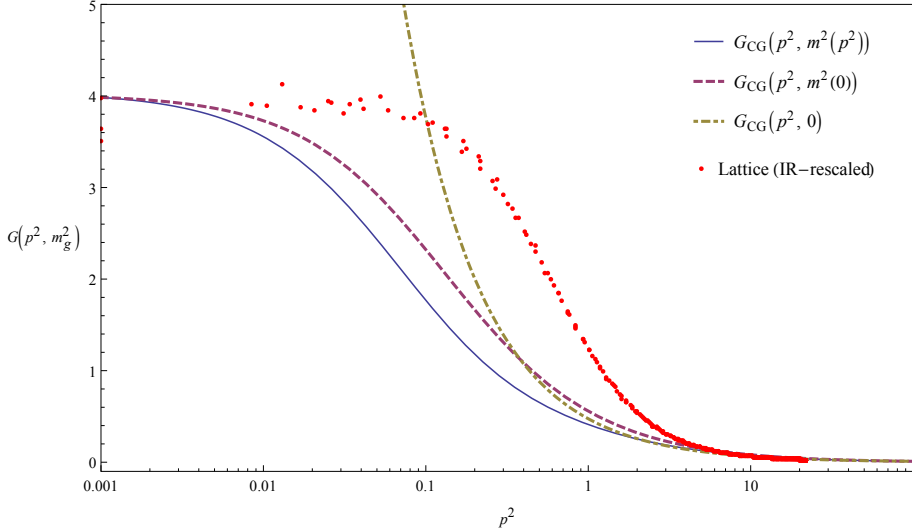


Figure 5.8: Comparison of our CG results for the gluon propagator with dynamical and constant gluon mass to the (massless 1-loop) perturbative result, and to lattice data rescaled in the IR.  $p^2$  is in  $GeV^2$  units,  $\mu_1 = 100GeV^2$ ,  $m = 500MeV$ , and  $r = 2$ .

We see that, with this rescaling, the contrast between the 1-effective-loop and the lattice results is similar to the contrast between SDE and the same lattice ones shown in Fig.3.6, where the freezing of the SDE solution is constrained to equal the original corresponding lattice value. This means that our 1-effective-loop result does approximate the full, PT-SDE one – either in BFG or CG, as noted in Sect.5.2 – as well as the usual perturbative one in the UV, and therefore is a positive result.

We should also explore, for matters of investigation, rescaling the lattice data according to the other renormalization condition, the one in the UV, approximating the lattice to our high-energy behavior. This leads to the graphs in Figs.5.9,5.10:

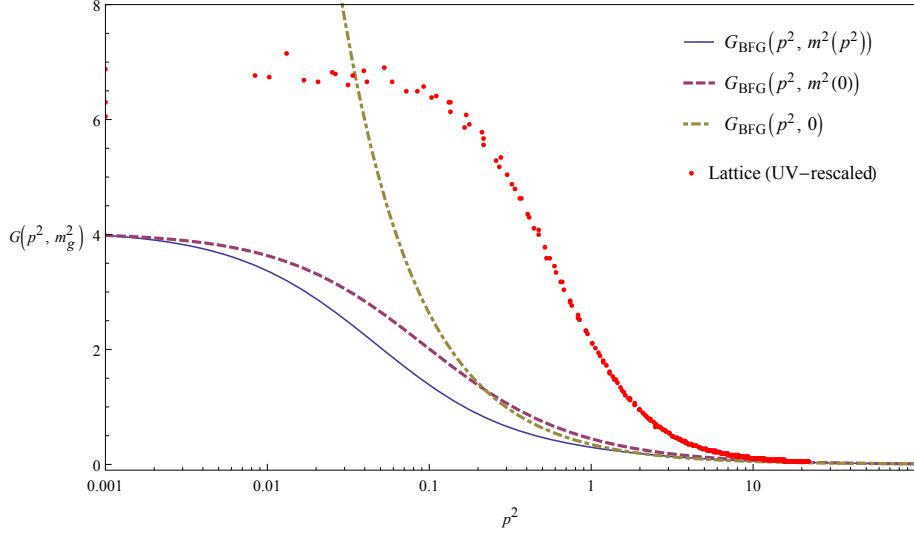


Figure 5.9: Comparison of our BFG results for the gluon propagator with dynamical and constant gluon mass to the (massless 1-loop) perturbative result, and to lattice data rescaled in the UV.  $p^2$  is in  $GeV^2$  units,  $\mu_1 = 100GeV^2$ ,  $m = 500MeV$ , and  $r = 2$ .

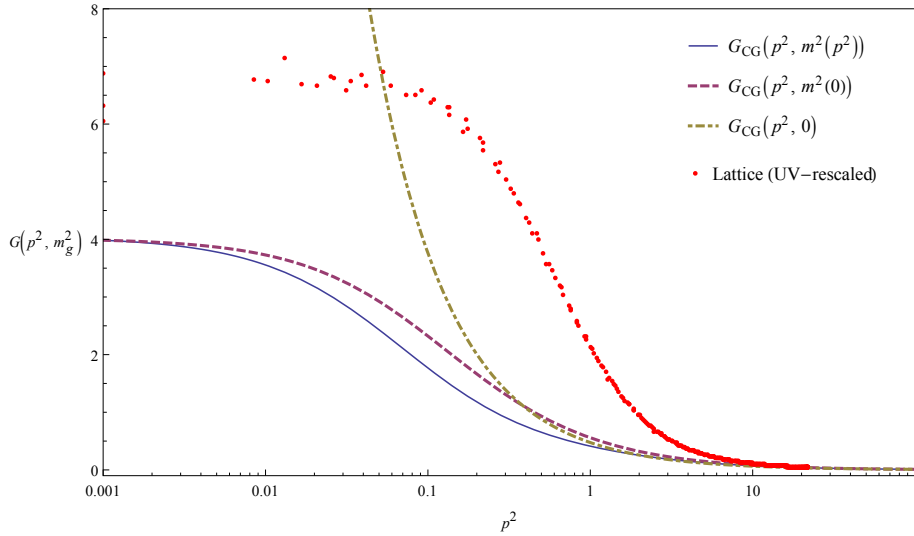


Figure 5.10: Comparison of our CG results for the gluon propagator with dynamical and constant gluon mass to the (massless 1-loop) perturbative result, and to lattice data rescaled in the UV.  $p^2$  is in  $GeV^2$  units,  $\mu_1 = 100GeV^2$ ,  $m = 500MeV$ , and  $r = 2$ .

In this case, the 1-effective-loop gluon propagator is definitely too suppressed comparing with the lattice.

While this can point to the IR-rescaling of the lattice as a better approach for comparison with lattice, the situation for the ghost dressing function is not that resolved.

### 5.3.2 Ghost dressing

On one hand, there is no IR condition imposed on the ghost dressing, which led to quite distinct freezing values for  $F$ , as discussed in Sect.5.2. On the other, we have also noted, with Figs.5.2,5.6, that such difference did not lead to much distinct ghost propagators  $F(p)/p^2$ . This means that an analysis in terms of the dressing function accentuates the differences among the lattice, the 1-effective-, and the 1-usual-loop results.

Since the IR rescaling of the lattice was well-succeeded for the gluon propagator, we explored doing the same for the ghost dressing, rescaling the lattice data at lowest momentum to be close to our freezing values for  $F$ . This led to Fig.5.11 below, showing that this is not a good procedure for the dressing.

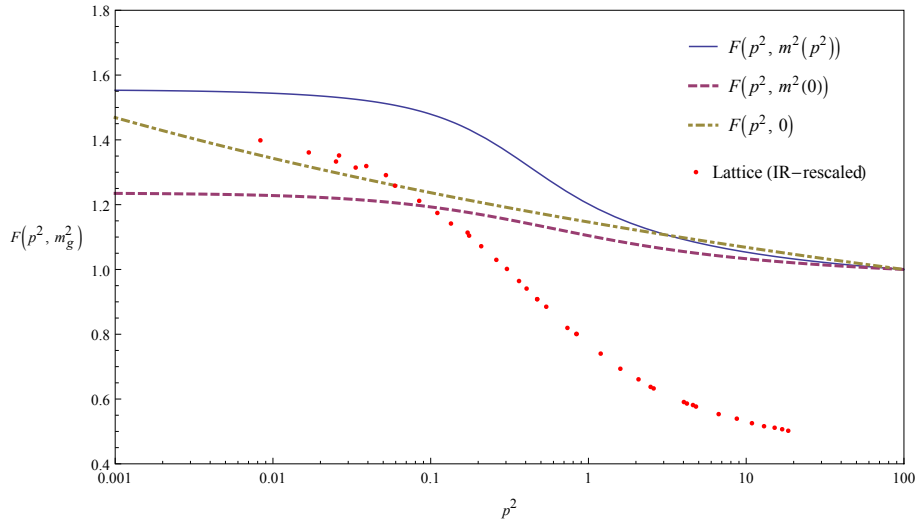


Figure 5.11: Comparison of our results for the ghost dressing with dynamical and constant gluon mass to the (massless 1-loop) perturbative result, and to lattice data rescaled in the IR.  $p^2$  is in  $GeV^2$  units,  $\mu = 100GeV^2$ ,  $m = 500MeV$ , and  $r = 2$ .

Now, rescaling the lattice values to the UV limit of our result led to Fig.5.12:

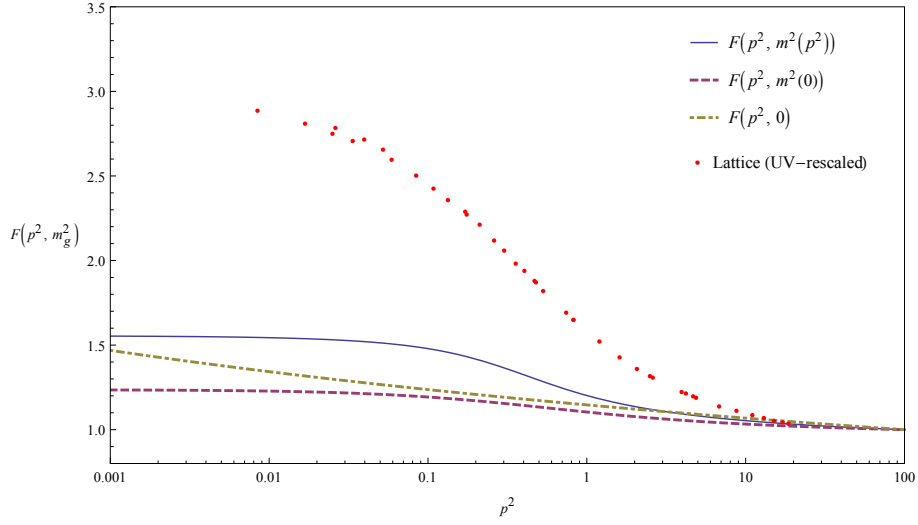


Figure 5.12: Comparison of our results for the ghost dressing with dynamical and constant gluon mass to the (massless 1-loop) perturbative result, and to lattice data rescaled in the UV.  $p^2$  is in  $GeV^2$  units,  $\mu = 100GeV^2$ ,  $m = 500MeV$ , and  $r = 2$ .

This is surely better, but, like in Figs.5.9,5.10 for the gluon propagator, it is too IR suppressed compared with the UV-rescaled lattice.

It seems, then, that an intermediate rescaling of the lattice may be better – still not satisfactory, though: our result is still IR suppressed, while the lattice becomes remarkably lower than ours in the perturbative limit<sup>‡</sup>, as shown in Fig.5.13:

---

<sup>‡</sup>The difference in the UV limits is however quite similar to the difference between the three  $F(p^2, m^2(p^2))$ ,  $F(p^2, m^2(0))$ ,  $F(p^2, 0)$  for  $p > \mu$ .



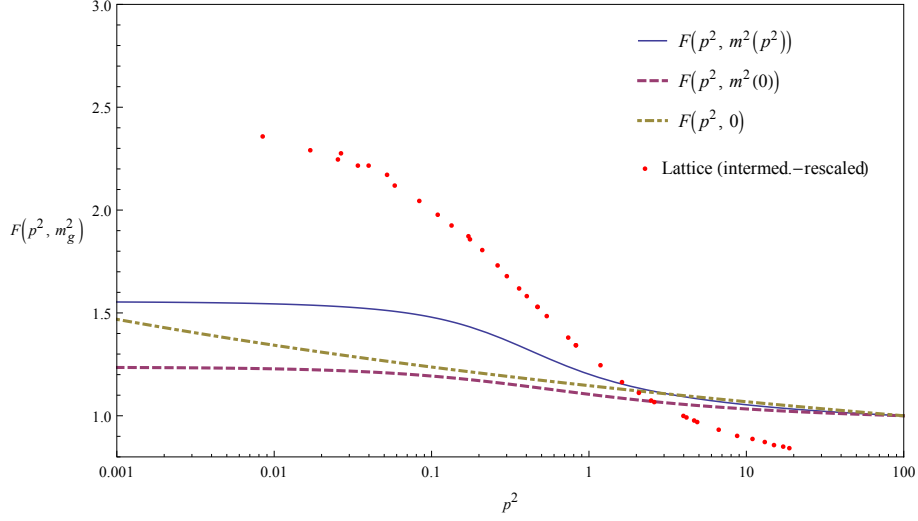


Figure 5.13: Comparison of our results for the ghost dressing, with dynamical and constant gluon mass, to the respective (massless 1-loop) perturbative and lattice ones. The latter is rescaled by a factor 2,  $p^2$  is in  $GeV^2$  units,  $\mu = 100GeV^2$ ,  $m = 500MeV$ , and  $r = 2$ .

If we apply this same rescaling to the data for the ghost propagator, the comparison looks better, as shown in Fig.5.14:

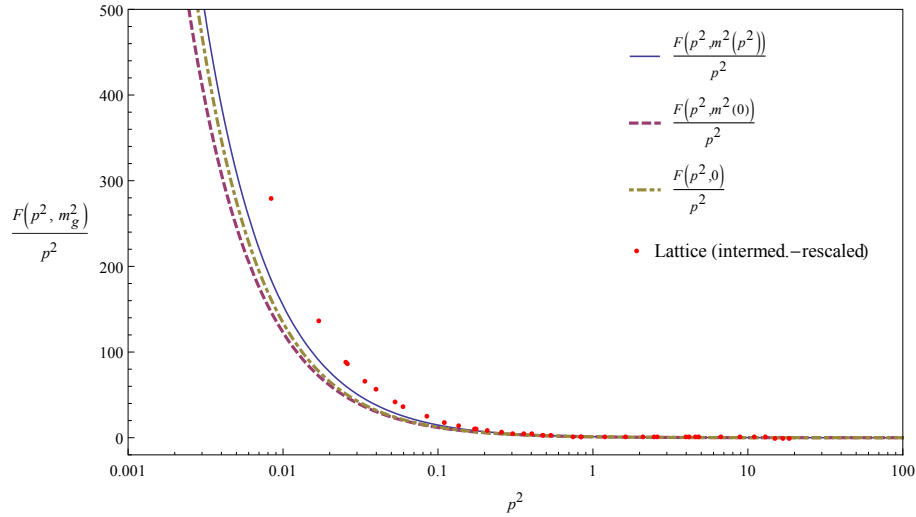


Figure 5.14: Comparison of our results for the ghost propagator, with dynamical and constant gluon mass, to the respective (massless 1-loop) perturbative and lattice ones. The latter is rescaled by a factor 2,  $p^2$  is in  $GeV^2$  units,  $\mu = 100GeV^2$ ,  $m = 500MeV$ , and  $r = 2$ .

## 5.4 Conclusions and prospects

Our results have shown that the desired method of effective loops is, first of all, still likely to require further ingredients – as the rescaling of lattice data for the analysis, which we consider still not enough for suggesting an univocal successful procedure. Comparison to other lattice results, including  $SU(2)$  YM and possibly other gauges, as well as calculation of more correlation functions, may clarify this situation and further probe the effectiveness of our approximations.

Nevertheless, the results do display the IR qualitative behavior indicated by purely nonperturbative studies for these propagators in the Landau gauge. At this point of the proposal, this, together with the transversality of the background gluon propagator and that  $\zeta_{\perp \theta=0}^{CG} \approx \zeta_{\perp \theta=1}^{BFG} \equiv \zeta_{\theta=1}^{BFG}$ , stands as some success for the employment of the three-gluon vertex dressing, the effective charge (3.4), and specially the RPT renormalization approach.

Concerning the correlation functions still, the three-gluon vertex will soon be calculated, so its 1-effective-loop result can also be compared with its dressing employed in the effective-loop expansion. That is, besides comparing with lattice, the results can be contrasted with the very expression inserted in the loops, that was chosen to be dressed or not. This would tell if the scheme is *approximately* consistent<sup>§</sup> as an 1 loop truncation, yet able to access deeper into the IR domain of the theory.

This framework, together with the *Mathematica* code, is readily applicable to further cases: from YM vertices to the inclusion of quarks, in general gauges and general momentum configurations. These calculations will provide further material for analysis and comparison to lattice, so as to evolve the understanding of limitations and the effectiveness of the method proposed.

Renormalization group analyses are also intended and, after the improvement to full QCD, some first phenomenological applications are also planned for Post-Doctorate research.

---

<sup>§</sup>As opposed to an actual SDE solution, which is self-consistent by construction.

# Appendix A

## Summary of the calculation procedure

This appendix briefly describes the logic followed by the *Mathematica* code constructed, for the case of propagators.

It begins by distinguishing the terms of the following form:

$$\frac{n_{\alpha\beta ab}(p, l)}{\left((p-l)^2 + am^2\right)^\alpha (l^2 + bm^2)^\beta}, \quad (\text{A.1})$$

specified by  $(\alpha\beta ab)$ , for each  $\alpha, \beta \geq 0, a, b = 0, 1$ . Here,  $n_{\alpha\beta ab}$  denotes the numerator corresponding to each of these denominators.

Each  $n_{\alpha\beta ab}$  is a function of the external and the loop momentum,  $p$  and  $l$ , respectively. After the proper Feynman parametrization and accompanying change of variables\*, we apply to  $n$  the usual loop integration properties – such as, for example†:

$$(p.l)^n \mapsto \begin{cases} 0 & \text{for odd } n \\ (p^2 l^2 / D)^{n/2} & \text{for even } n \end{cases} \quad (\text{A.2})$$

so that it ends up as a polynomial in  $l^2$ :

$$n_{\alpha\beta ab}(p, l) \mapsto \bar{n}_{\alpha\beta ab}(p^2, l^2, x) = \sum_{\lambda=0}^{\lambda_{\text{sup}}} C_{\alpha\beta ab}^{(\lambda)}(p^2, x) (l^2)^\lambda, \quad (\text{A.3})$$

where  $x$  is the Feynman parameter and, by construction,

$$C_{\alpha\beta ab}^{(\lambda)}(p^2, x) = \frac{1}{\lambda!} \left. \frac{d^\lambda \bar{n}_{\alpha\beta ab}}{d(l^2)^\lambda} \right|_{l^2=0}. \quad (\text{A.4})$$

Each of these coefficients will be, then, the coefficient of each loop integral

$$\frac{1}{\nu^{D-4}} \int \frac{d^D l}{(2\pi)^D} \frac{(l^2)^\lambda}{(l^2 + \Delta)^{\alpha+\beta}} =: \text{int}(\alpha, \beta, a, b, \lambda), \quad (\text{A.5})$$

---

\*For the  $\alpha, \beta \neq 0$  case, for instance, it is  $l \mapsto l - xp$ .

†Similar relations with tensor indices are defined as well. Also,  $D$  is the spacetime dimension.

where

$$\text{int}(\alpha > 0, \beta > 0, a, b, \lambda) \equiv \frac{1}{16\pi^2} \frac{\Gamma(\lambda + D/2)}{\Gamma(D/2)} \left( \frac{\Delta}{4\pi\nu^2} \right)^{-2+D/2} \Delta^{2+\lambda-\alpha-\beta} \Gamma(\alpha + \beta - \lambda - D/2), \quad (\text{A.6})$$

and  $\Delta \equiv \Delta(\alpha > 0, \beta > 0, a, b) = x(1-x)p^2 + (xa + (1-x)b)m^2$ .

So, the sum of the integrals (A.6), with coefficients (A.4) and the additional Feynman-parametrization factor

$$\text{den}(\alpha > 0, \beta > 0) := \frac{x^{\alpha-1}(1-x)^{-1}}{\Gamma(\alpha)\Gamma(\beta)} \quad (\text{A.7})$$

yield the contribution of all terms (A.1) with  $\alpha, \beta > 0$ .

Similar procedure is done for the cases  $(\alpha = 0, \beta > 0)$  and  $(\alpha > 0, \beta = 0)$ , with corresponding Feynman parametrization and definitions for the functions  $\text{den}(\alpha, \beta)$  and  $\text{int}(\alpha, \beta, a, b, \lambda)$ . Summarizing, we have

$$\frac{n_{\alpha\beta ab}(p, l)}{((p-l)^2 + am^2)^\alpha (l^2 + bm^2)^\beta} \xrightarrow{\int d^D l} \text{den}(\alpha, \beta) \sum_{\lambda=0}^{\lambda_{\text{sup}}} C_{\alpha\beta ab}^{(\lambda)}(p^2, x) \text{int}(\alpha, \beta, a, b, \lambda), \quad (\text{A.8})$$

where  $C_{\alpha\beta ab}^{(\lambda)}$  is in either case given by (A.4).

The results for all  $(\alpha, \beta, a, b)$  are summed up, and the sum is then expanded around  $D = 4$ , and finally the integration over the Feynman parameter gives the final result.

## Bibliography

- [1] K.A. Olive et al. (Particle Data Group), *Chin. Phys. C*, 38, 090001 (2014).
- [2] Eisberg, R. M. *Fundamentals of Modern Physics* . John Wiley & Sons, Inc. 1961.
- [3] Tomonaga, S. *Quantum Mechanics* . Interscience Publishers. 1962.
- [4] Schwabl, F. *Advanced Quantum Mechanics* . 3rd ed. Springer. 2005.
- [5] Griffiths, D. *Introduction to Elementary Particles* . John Wiley & Sons, Inc. 1987.
- [6] Perkins, D. H. *Introduction to High Energy Physics* . 3rd ed. Addison Wesley. 1987.
- [7] Bogoliubov, N. N.; Shirkov, D. V. *Introduction to the Theory of Quantized Fields*. 3rd ed. John Wiley & Sons Inc. 1980. N.P. Konopleva, V.N. Popov, *Gauge Fields*. Routledge, 1982.
- [8] E. Noether, "Invariant Variation Problems". *Transport Theory and Statistical Physics* 1 (3): 186207.
- [9] Aitchinson, I. J. R.; Hey, A. J. G. *Gauge Theories in Particle Physics*. Graduate Student Series in Physics. Adam Hilger Ltd. 1982.
- [10] H. Pagels and S. Stokar, *Phys. Rev. D* 20, 2947 (1979).
- [11] J. M. Cornwall, *Phys. Rev. D* 26, 1453 (1982).
- [12] J. M. Cornwall, *Phys.Rev. D*80 (2009) 096001. A.C. Aguilar,, J. Papavassiliou, *Eur.Phys.J. A*31 (2007) 742-745. A. C. Aguilar, D. Binosi, J. Papavassiliou, *PoS LC2008*, 050 (2008). J. M. Cornwall, W.-S. Hou, *Phys.Rev. D*34 (1986) 585.

- [13] A. A. Natale, *Braz.J.Phys.* 37 (2007) 306-312. A. A Natale, *PoS QCD-TNT09* (2009) 031; hep-ph/0910.5689v1. A.C. Aguilar, A. Mihara, A.A. Natale *Phys.Rev. D65* (2002) 054011.
- [14] F. A. Machado, A. A. Natale, *AIP Conf. Proc.* 1520, 343 (2013).
- [15] F. A. Machado, A. A. Natale, to appear.
- [16] A. Doff, F.A. Machado, A.A. Natale, *Annals Phys.* 327 (2012) 1030-1049.
- [17] A. Doff, F.A. Machado, A.A. Natale, *New J.Phys.* 14 (2012) 103043.
- [18] J. M. Cornwall, *Phys.Rev. D83* (2011) 076001.
- [19] Itzykson, C.; Zuber, J-B. *Quantum Field Theory.* McGraw-Hill. 1980.
- [20] Ryder, L. H. *Quantum Field Theory.* 2nd ed. Cambridge University Press. 1996.
- [21] Coleman, S. *Aspects of Symmetry.* Cambridge University Press. 1988.
- [22] Zee, A. *Quantum Field Theory in a Nutshell.* Princeton University Press. 2003.
- [23] H. Lehmann, K. Symanzik, and W. Zimmermann, *Nuovo Cimento* 1, 205 (1955).
- [24] Muta, T. *Foundations of Quantum Chromodynamics: An Introduction to Perturbative Methods in Gauge Theories.* World Scientific Pub Co Inc. 1987.
- [25] Pokorski, S. *Gauge Field Theories.* 2nd ed. Cambridge Monographs on Mathematical Physics. Cambridge University Press. 2000.
- [26] J. Greensite, *Prog.Part.Nucl.Phys.* 51 (2003) 1. M. Engelhardt, *Nucl.Phys.Proc.Suppl.* 140 (2005) 92-105.
- [27] S. Weinberg, *The Quantum Theory of Fields, Volume 2: Modern Applications.* Cambridge University Press. 2005.
- [28] J. C. Collins, *Renormalization: An Introduction to Renormalization.* Cambridge Monographs on Mathematical Physics. Cambridge University Press. 1986.
- [29] D.J. Gross, F. Wilczek . *Phys.Rev.Lett.* 30 (1973) 1343-1346. D.J. Gross, *Nucl.Phys.Proc.Suppl.* 74 (1999) 426-446.
- [30] Marciano, W.; Pagels, H. *Quantum Chromodynamics.* *Physics Reports* 36, 3 (1978) 137-276.

- [31] J.D. Bjorken, Phys.Rev. 179 (1969) 1547-1553.
- [32] C. Lorcé. Lectures at the Second Int. Summer School of the GDR PH-QCD, Orsay. Available at [indico.in2p3.fr/event/9917/contribution/25/material/slides/](http://indico.in2p3.fr/event/9917/contribution/25/material/slides/). J.C. Collins, Acta Phys. Polon. B34, 3103 (2003).
- [33] J. C. Collins, Foundations of Perturbative QCD. Cambridge Monographs on Particle Physics, Nuclear Physics and Cosmology. Cambridge University Press. 2013.
- [34] T. van Ritbergen, J.A.M. Vermaseren, S.A. Larin, Phys. Lett. B 400, 379 (1997).
- [35] M. Cacciari, N. Houdeau, JHEP 09 (2011) 039.
- [36] Cahn, R. N.; Goldhaber, G.E. The Experimental Foundations of Particle Physics. 1st ed. Cambridge University Press. 1991. Sterman, G. QCD and Jets. arXiv:hep-ph/0412013v1 (2004). Webber, B. R. Fragmentation and Hadronization. arXiv:hep-ph/9912292v1 (1999).
- [37] R. Hirosky, PSNUM-09 C12-09-12, p.65-78.
- [38] M. Peskin, Lectures at Les Houches Sum.School 1982:217, SLAC-PUB-3021. Alkofer, R.; Von Smekal, L. The infrared behaviour of QCD Green's functions: Confinement, dynamical symmetry breaking, and hadrons as relativistic bound states. Physics Reports 353, 5-6 (2001) 281-465.
- [39] S. Narison, QCD as a Theory of Hadrons: From Partons to Confinement. Cambridge Monographs on Particle Physics, Nuclear Physics and Cosmology. Cambridge University Press. 2007.
- [40] A. Cucchieri, T. Mendes, PoS LATTICE2010 (2010) 280, and references therein.
- [41] V. N. Gribov, Nucl.Phys. B139 (1978) 1. D. Zwanziger, Nucl.Phys. B412 (1994) 657-730.
- [42] D. Dudal, N. Vandersickel, H. Verschelde, S.P. Sorella, PoS QCD-TNT09 (2009) 012. D. Dudal, S.P. Sorella, N. Vandersickel, Phys.Rev. D84 (2011) 065039. D. Dudal, N. Vandersickel, L. Baulieu, S.P. Sorella, M.S. Guimaraes, M.Q. Huber, O., D. Zwanziger, PoS LC2010 (2010) 021.

- [43] A. V. Manohar, Lect.Notes Phys. 479 (1997) 311-362, and references therein.
- [44] Mandelstam, S., Phys. Rev. D 20, 12 (1979) 3223–3238.
- [45] Brown, N.; Pennington, M. R., Phys. Rev. D 38, 7 (1988) 2266–2276.
- [46] Aguilar, A. C. Geração de Massa em Teorias de Gauge. 2004. Tese de Doutorado – Instituto de Física Teórica, Universidade Estadual Paulista.
- [47] Huang, K. Quarks, Leptons and Gauge Fields. World Scientific Pub Co Inc. 1992.
- [48] Cudell, J. R.; Ross, D. A., Nuclear Physics B 359, 2-3 (1991) 247-261. Von Smekal, L.; Hauck, A.; Alkofer, R., Phys. Rev. Lett. 79, 19 (1997) 3591–3594. Aguilar, A. C.; Natale, A. A. Int. J. Mod. Phys. A 20 (2005) 7613-7632. Aguilar, A. C.; Papavassiliou, J. Eur. Phys. J. A 31, 742-745 (2007). Aguilar, A. C.; Binosi, D.; Papavassiliou, J. Phys. Rev. D 78, 025010 (2008).
- [49] Bernard, C.; Parrinello, C.; Soni, A., Phys. Rev. D 49, 3 (1994) 1585–1593. Leinweber, D. B.; Skullerud, J. I.; Williams, A.G.; Parrinello, C., Phys. Rev. D 58, 031501(R) (1998). Bonnet, F. D. R. *et al.* Phys. Rev. D 62, 051501(R) (2000). Bonnet, F. D. R. *et al.* Phys. Rev. D 64, 034501 (2001). Alexandrou, C.; De Forcrand, Ph.; Follana, E., Phys. Rev. D 65, 114508 (2002). Alexandrou, C.; De Forcrand, Ph.; Follana, E., Phys. Rev. D 65, 117502 (2002). Bloch, J. C. R.; Cucchieri, A.; Langfeld, K.; Mendes, T., Nuclear Physics B - Proceedings Supplements 119 (2003) 736-738. Boucaud, P. *et al.* Phys. Rev. D 70, 034509 (2004). Sternbeck, A.; Ilgenfritz, E.-M.; Müller-Preussker, M., Phys. Rev. D 72, 014507 (2005). Sternbeck, A.; Ilgenfritz, E.-M.; Müller-Preussker, M., Phys. Rev. D 73, 014502 (2006). Boucaud, P. *et al.* JHEP06(2006). Bowman, P. O. *et al.* Phys. Rev. D 76, 094505 (2007). Cucchieri, A.; Mendes, T., Phys. Rev. Lett. 100, 241601 (2008). Cucchieri, A.; Mendes, T., Phys. Rev. D 81, 016005 (2010).
- [50] A. C. Aguilar, D. Binosi and J. Papavassiliou, Phys. Rev. D 78, 025010 (2008).
- [51] A.C. Aguilar, A.A. Natale, JHEP 0408 (2004) 057.
- [52] I.L. Bogolubsky, E.M. Ilgenfritz, M. Muller-Preussker, A. Sternbeck, PoS LAT2007 (2007) 290.
- [53] A.C. Aguilar, D. Binosi, J. Papavassiliou, Phys.Rev. D89 (2014) 085032. A.C. Aguilar, D. Binosi, J. Papavassiliou, Phys.Rev. D84 (2011) 085026. A.C. Aguilar, J. Papavassiliou, Eur.Phys.J. A35 (2008) 189-205.



- [54] Slavnov, A A (1972). *Theor.Math.Phys.* 10: 99.
- [55] D. Binosi, J. Papavassiliou, *Phys.Rept.* 479 (2009) 1-152.
- [56] E. S. Swanson, J. Meyers, *Phys.Rev. D* 90 (2014) 045037, and references therein.
- [57] A. Cucchieri, Proc. C02-04-14.1, p.137-146; hep-lat/0209076. E.-M. Ilgenfritz, M. Muller-Preussker, A. Sternbeck, A. Schiller Proc. C06-01-26; hep-lat/0601027. P. Boucaud, J.P. Leroy, A. Le Yaouanc, A.Y. Lokhov, J. Micheli, O. Pene, J. Rodriguez-Quintero, C. Roiesnel, hep-ph/0507104. A.C. Aguilar, D. Binosi, J. Papavassiliou, *JHEP* 1007 (2010) 002.
- [58] Yu. L. Doshitzer, Talk given at 29th International Conference on High-Energy Physics (ICHEP 98), Vancouver, Canada, 23-29 Jul 1998, In “Vancouver 1998, High Energy Physics”, vol. 1 305-324, hep-ph/9812252.
- [59] D. Binosi and J. Papavassiliou, *Phys. Rev. D* 66, 111901 (2002); *Nucl. Phys. Proc. Suppl.* 121, 281 (2003); *J. Phys. G* 30, 203 (2004); *Nucl. Phys. Proc. Suppl.* 133, 281 (2004); *JHEP* 0703, 041 (2007); *Phys. Rev. D* 77, 061702 (2008); *JHEP* 0811, 063 (2008).
- [60] A. C. Aguilar, J. Papavassiliou, *JHEP* 0612 (2006) 012.
- [61] L.F. Abbott, *Acta Phys.Polon.* B13 (1982) 33. L.F. Abbott, *Nucl.Phys.* B185 (1981) 189.
- [62] A. Denner, G. Weiglein, S. Dittmaier, *Phys. Lett. B*, 333 420 (1994).
- [63] A. Pilaftsis, *Nucl.Phys.* B487 (1997) 467-491.
- [64] D. V. Shirkov and I. L. Solovtsov, *Phys. Rev. Lett.* 79, 1209 (1997).
- [65] P. V. Landshoff and O. Nachtmann, *Z. Phys. C* 35, 405 (1987); A. Donnachie and P. V. Landshoff, *Nucl. Phys. B* 231, 189 (1984).
- [66] A. C. Aguilar, A. A. Natale and P. S. Rodrigues da Silva, *Phys. Rev. Lett.* 90, 152001 (2003).
- [67] D. V. Shirkov, *Phys. Atom. Nucl.* 62, 1928 (1999) [*Yad. Fiz.* 62, 2082 (1999)].
- [68] D. V. Shirkov and I. L. Solovtsov, *Theor. Math. Phys.* 150, 132 (2007).
- [69] S. J. Brodsky, E. Gardi, G. Grunberg and J. Rathsman, *Phys. Rev. D* 63, 094017 (2001).

- [70] J. R. Forshaw, J. Papavassiliou and C. Parrinello, Phys. Rev. D 59, 074008 (1999).
- [71] F. Halzen, G. I. Krein and A. A. Natale, Phys. Rev. D 47 , 295 (1993); M. B. Gay Ducati, F. Halzen and A. A. Natale, Phys. Rev. D 48 , 2324 (1993); A. C. Aguilar, A. Mihara and A. A. Natale, Phys. Rev. D 65 , 054011 (2002); E. G. S. Luna, A. F. Martini, M. J. Menon, A. Mihara and A. A. Natale, Phys. Rev. D 72 , 034019 (2005); E. G. S. Luna and A. A. Natale, Phys. Rev. D 73 , 074019 (2006); E. G. S. Luna, Phys. Lett. B. 641 , 171 (2006).
- [72] A. C. Aguilar, D. Ibáñez, and J. Papavassiliou, Phys. Rev. D 87 , 114020 (2013), and references therein.
- [73] J. M. Cornwall, C12-09-03.11; hep-ph/1211.2019.
- [74] J.C.R. Bloch, A. Cucchieri, K. Langfeld, T. Mendes, Nucl.Phys. B687 (2004) 76-100, and references therein.
- [75] E.-M. Ilgenfritz, M. Muller-Preussker, A. Sternbeck, A. Schiller, I.L. Bogolubsky, Braz.J.Phys. 37 (2007) 193-200.